Published in "Paleoceanography 31(10): 1350–1367, 2016"
which should be cited to refer to this work.

Environmental constraints on Holocene cold-water coral reef growth off Norway: Insights from a multiproxy approach

Jacek Raddatz[1,2], Volker Liebetrau[2], Julie Trotter[3], Andres Rüggeberg[4,5], Sascha Flögel[2], Wolf-Christian Dullo[2], Anton Eisenhauer[2], Silke Voigt[1], and Malcolm McCulloch[3,6]

[1]Goethe University Frankfurt, Institute of Geosciences, Frankfurt am Main, Germany, [2]GEOMAR Helmholtz Centre for Ocean Research Kiel, Kiel, Germany, [3]The UWA Oceans Institute and School of Earth and Environment, University of Western Australia, Crawley, Western Australia, Australia, [4]Renard Centre of Marine Geology, Department of Geology and Soil Sciences, Ghent University, Gent, Belgium, [5]Department of Geosciences, University of Fribourg, Fribourg, Switzerland, [6]ARC Centre of Excellence in Coral Reef Studies, University of Western Australia, Crawley, Western Australia, Australia

Key Points:
- Multiproxy approach in *Lophelia pertusa* reveals changes in seawater properties throughout the Holocene
- Coupled boron isotopes and U/Ca approach
- CWC reef decline due to advances of Arctic waters

Correspondence to:
J. Raddatz,
raddatz@em.uni-frankfurt.de

Citation:
Raddatz, J., V. Liebetrau, J. Trotter, A. Rüggeberg, S. Flögel, W.-C. Dullo, A. Eisenhauer, S. Voigt, and M. McCulloch (2016), Environmental constraints on Holocene cold-water coral reef growth off Norway: Insights from a multiproxy approach, *Paleoceanography*, *31*, 1350–1367, doi:10.1002/2016PA002974.

Abstract High-latitude cold-water coral (CWC) reefs are particularly susceptible due to enhanced CO_2 uptake in these regions. Using precisely dated (U/Th) CWCs (*Lophelia pertusa*) retrieved during research cruise POS 391 (Lopphavet 70.6°N, Oslofjord 59°N) we applied boron isotopes ($\delta^{11}B$), Ba/Ca, Li/Mg, and U/Ca ratios to reconstruct the environmental boundary conditions of CWC reef growth. The sedimentary record from these CWC reefs reveals a lack of corals between ~6.4 and 4.8 ka. The question remains if this phenomenon is related to changes in the carbonate system or other causes. The initial postglacial setting had elevated Ba/Ca ratios, indicative of meltwater fluxes showing a decreasing trend toward cessation at 6.4 ka with an oscillation pattern similar to continental glacier fluctuations. Downcore U/Ca ratios reveal an increasing trend, which is outside the range of modern U/Ca variability in *L. pertusa*, suggesting changes of seawater pH near 6.4 ka. The reconstructed bottom water temperature at Lopphavet reveals a striking similarity to Barent sea surface and subsea surface temperature records. We infer that meltwater pulses weakened the North Atlantic Current system, resulting in southward advances of cold and CO_2-rich Arctic waters. A corresponding shift in the $\delta^{11}B$ record from ~25.0‰ to ~27.0‰ probably implies enhanced pH up-regulation of the CWCs due to the higher pCO_2 concentrations of ambient seawater, which hastened mid-Holocene CWC reef decline on the Norwegian margin.

1. Introduction

Cold-water coral (CWC) reefs on the European continental margin are hot spots of marine biodiversity, but due to ongoing climate change, they are under serious threat [*Guinotte et al*., 2006; *Roberts and Cairns*, 2014]. In particular, the current rise in atmospheric carbon dioxide concentrations (CO_2) dissolves into the oceans and therefore leads to a decrease in seawater pH, known as "ocean acidification" [e.g., *Doney et al*., 2009]. This phenomenon probably limits the growth and survival of cold-water corals due to shoaling of the aragonite saturation horizon (ASH, aragonite saturation state = $\Omega_{arag} = [Ca^{2+}][CO_3^{2-}]/K^*_{arag}$, where K^*_{arag} is the stoichiometric solubility product of aragonite). Given their proximity to the carbonate saturation horizon, CWCs are particularly vulnerable to the impact of climate change and the consequent effects on seawater chemistry [*Guinotte et al*., 2006]. The main framework builder of CWC reefs in the NE Atlantic is *Lophelia pertusa* [*Linnaeus*, 1758 (*Desmophyullum pertusum* [*Addamo et al*., 2016; *Freiwald et al*., 2004, Figure 1]). Single *L. pertusa* polyps can be found within a seawater temperature range of 4–14°C [*Freiwald et al*., 2004, 2009; *Roberts et al*., 2006] with only a few exceptions in the western Atlantic [*Mienis et al*., 2014], whereas flourishing reefs thrive between >6°C on the Norwegian margin and <10°C on the Irish margin [*Flögel et al*., 2014]. Possibly even more important is their dependency on the state of the ocean carbonate system to survive and flourish [*Flögel et al*., 2014; *Guinotte et al*., 2006]. Considering the apparent relationship of flourishing CWC reefs on the European continental margin to seawater density (sigma theta $\sigma_\theta = 27.5 \pm 0.15$ [*Dullo et al*., 2008; *Rüggeberg et al*., 2011]), flourishing reefs appear to be abundant in seawater with a dissolved inorganic carbon concentration of 2170 (μmol/kg) and pH between 7.98 and 8.3, implying a strong dependency of CWC reef growth on the carbonate chemistry of ambient seawater [*Flögel et al*., 2014], whereas single *L. pertusa* polyps are able to survive cultivation studies under a

pH of 7.4 [*Form and Riebesell*, 2012]. Recent studies have demonstrated by the use of boron isotope systematics ($\delta^{11}B$) that CWCs are resilient (to some extent) to changing seawater carbonate chemistry, by regulating their internal pH to sustain calcification [*Anagnostou et al*., 2012; *Martin et al*., 2016; *McCulloch et al*., 2012; *Trotter et al*., 2011; *Wall et al*., 2015]. This phenomenon appears to be consistent with culturing experiments [*Form and Riebesell*, 2012].

On geological time scales the initiation, development, and demise of CWC reefs have been sensitive to various oceanographic parameters such as bottom currents, nutrient availability/sea surface productivity, and water mass stratification [e.g., *Eisele et al*., 2011; *Hebbeln et al*., 2016; *Kano et al*., 2007; *Raddatz et al*., 2011, 2014a; *Rüggeberg et al*., 2007, 2016]. Particularly, CWC growth in the NE Atlantic reveals a distinct shift of the biogeographic limit from high to low latitudes in glacial periods [*Eisele et al*., 2011; *Frank et al*., 2004, 2009, 2011; *McCulloch et al*., 2010; *Wienberg et al*., 2009, 2010]. During interglacial periods (Holocene) CWC reef growth was predominantly restricted to the Norwegian and Irish margins as well as to the Bay of Biscay [*Eisele et al*., 2008; *Dorschel et al*., 2005; *Rüggeberg et al*., 2007, 2016; *Frank et al*., 2009], whereas CWC reef growth off Mauretania and in the Gulf of Cadiz occurred mostly during glacial periods [*Eisele et al*., 2011; *Frank et al*., 2011; *Wienberg et al*., 2010]. Such an obviously climatically driven pattern of active CWC reef growth has been primarily attributed to changes in sea surface productivity and movements of the Polar Front [*Frank et al*., 2011, and references therein]. However, CWC reef occurrences during the Holocene on the Norwegian margin appear to be driven by a more complex pattern than solely glacial/interglacial controlled growth from high to low latitudes [*López Correa et al*., 2012; *Stalder et al*., 2014; *Titschack et al*., 2015]. Combined U/Th and ^{14}C ages for a suite of CWC reefs reveal that Norwegian CWC reef growth may have declined during the mid-Holocene from ~7 to ~4 ka and for a slightly longer period within fjord systems from ~9 to ~4 ka [*López Correa et al*., 2012; *Titschack et al*., 2015]. However, a reasonable explanation for this observation remains to be determined.

Here we address this question by using well-dated (U/Th) CWCs and a multiproxy approach combining boron isotope systematics ($\delta^{11}B$) with elemental ratios (Li/Mg, U/Ca, and Ba/Ca ratios). This approach will help to reconstruct the environmental boundary conditions and the responses of CWC reefs growth during the Holocene.

2. Material and Methods

Sample material for this study has been recovered during research cruise POS 391 with R/V *Poseidon* off Norway in 2009 (Figure 1). Modern *L. pertusa* samples were either collected with the manned submersible JAGO of GEOMAR, Helmholtz Centre for Ocean Research Kiel (GEOMAR) (Lopphavet and Oslofjord) or with a Van-Veen grab (Sula reef). Gravity cores were taken after direct observations of the coral reef with the manned submersible, JAGO. The gravity cores were retrieved close to, but not within, the currently flourishing CWC reef at Lopphavet (between 70°26.6′N–70°28.9′N and 21°10.2′E–21°11.4′E, core numbers: 551-2, 551-3, 557-3, 559-2, and 559-3; Figures 1b and 1c) at depths from 226 to 268 m and in Oslofjord (59.08′ N, 19.5′E, core numbers: 575-2, 578-1, 576-1, and 576-2; Figures 1d and 1e) at 100 m water depth.

Sediment cores were frozen and cut before sampling to avoid sediment disturbances [*Dorschel et al*., 2005; *Foubert et al*., 2005]. Coral samples were then washed, rigorously mechanically cleaned with a dental drill, and subsequently cut for further sampling. In particular, longitudinal sections of *L. pertusa* were subsampled with a dental drill and a NewWave micromill avoiding the centers of calcification (COC) following *Rüggeberg et al.* [2008]. For two samples we also sampled the COC to characterize sample heterogeneity (429-11 versus 430-11 and 439-11 versus 440-11).

Samples were then split for X-ray diffraction (XRD) analyses, elemental ratios, boron isotope measurements, and U/Th dating. XRD measurements (>98% aragonite) indicate that all samples have retained their primary aragonite skeletons. Before subsampling for dating and elemental ratios, the fossil samples were chemically cleaning followed the protocol of *Cheng et al.* [2000a]; this protocol was not applied to samples prepared for boron isotope analysis. Furthermore, we did not employ alkaline diethylenetriamine-pentaacetic acid for barite removal, similar to other studies investigating Ba/Ca ratios in marine carbonates [e.g., *Bahr et al*., 2013; *Hönisch et al*., 2011, and references therein].

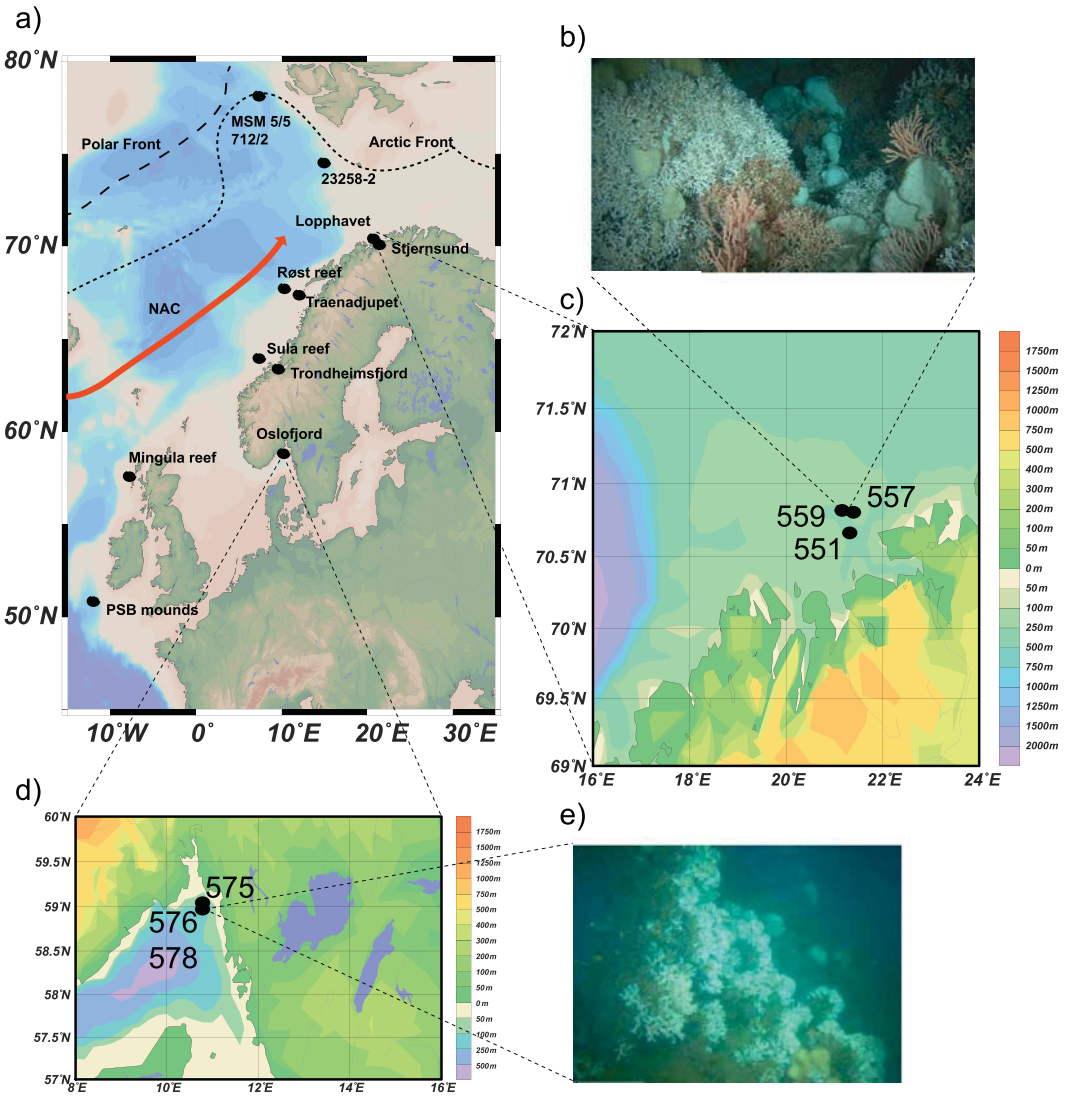

Figure 1. (a) Study location map of recent flourishing CWC reefs on the Norwegian margin, plus the Mingula reef complex and the Porcupine Seabight mounds are indicated. Recent Norwegian reefs are thriving in the North Atlantic Current (NAC). Also indicated are the Arctic and the Polar Front and important sites discussed in the paper MSM 5/5 712/2 [*Sørensen et al.*, 2014] and 23258-2 [*Sarnthein et al.*, 2003]. (b) In situ observation with the manned submersible JAGO during research cruise POS 391 of Lopphavet dive 1102. (c) Detailed map of coring sites at the Lopphavet reef. (d) Detailed map of the coring sites in the Oslofjord. (e) In situ observation with the manned submersible JAGO of the Oslofjord reef dive 1105. Maps are generated with ODV [*Schlitzer*, 2014].

2.1. U/Th Age Determinations

The uranium/thorium coral ages were performed on a VG Axiom multicollector inductively coupled plasma–mass spectrometer (MC-ICP-MS) at GEOMAR Helmholtz Centre for Ocean Research Kiel (Germany) following the protocols of *Fietzke et al.* [2005] and a quadrupole ICP-MS Agilent Series 7200cs (GEOMAR) according to the method of *Douville et al.* [2010]. Calculations ware based on decay constants of *Cheng et al.* [2000b]. The measurements were carried out with a combined $^{233/236}U/^{229}Th$ spike. The stock solutions were calibrated against National Institute of Standards and Technology Standard Reference Material (NIST-SRM) 3164 (U) and NIST-SRM 3159 (Th), as a combined spike calibrated against CRM-145 uranium standard solution for U-isotope compositions, and against a secular equilibrium standard (HU-1, uranium ore solution) for determination of $^{230}Th/^{234}U$ activity ratios. Full procedural blanks were around 60 pg for U, 6 to 9 pg for ^{232}Th, and 0.5 to 5 fg for ^{230}Th. A correction for detrital Th has been carried out, applying mean crustal composition values

Table 1. U/Th Geochronology of *Lophelia pertusa* Samples Retrieved During Research Cruise POS 391[a]

Lab Code				Location			MC = M
ICP-MS Type	Station Number/ Gear / Water Depth (m)	Core Depth (cm) Description	Sampling Region	Latitude (°N)	Longitude (°E)	U-Th Prepared Sample Aliqout (mg)	Quadr. = Q
M = MC. Q = Quadr							ICP-MS
429-11/M	550-1/JAGO/220	reef recent red	Lopphavet	70.61	21.22	49	M
808-13/Q	551-2/GC/244	6	Lopphavet	70.61	21.22	158	Q
439-11/M	551-3/GC/?	200	Lopphavet	70.61	21.22	50	M
809-13/Q	557-3/GC/268	1	Lopphavet	70.68	21.23	176	Q
809-13 wpr/Q	557-3/GC/268	1	Lopphavet	70.68	21.23	182	Q
497-12/M	559-2/GC/225	17	Lopphavet	70.69	21.23	39	M
497-12/Q	559-2/GC/225	17	Lopphavet	70.69	21.23	197	Q
810-13/M	559-2/GC/225	27	Lopphavet	70.69	21.23	54	M
811-13/M	559-2/GC/225	38	Lopphavet	70.69	21.23	25	M
812-13/Q	559-2/GC/225	56	Lopphavet	70.69	21.23	194	Q
813-13/Q	559-2/GC/225	86	Lopphavet	70.69	21.23	165	Q
814-13/Q	559-2/GC/225	103	Lopphavet	70.69	21.23	177	Q
816-13/Q	559-2/GC/225	184	Lopphavet	70.69	21.23	150	Q
816-13 wpr/Q	559-2/GC/225	184	Lopphavet	70.69	21.23	147	Q
817-13/Q	559-2/GC/225	221	Lopphavet	70.69	21.23	163	Q
818-13/Q	559-2/GC/225	235	Lopphavet	70.69	21.23	160	Q
819-13/Q	559-2/GC/225	1	Lopphavet	70.69	21.23	160	Q
820-13/Q	559-3/GC/237	8	Lopphavet	70.69	21.23	186	Q
433-11/M	559-3/GC/237	sed. surf./rec.	Sula	64.33	8.12	49	M
431-11/M	563-1/v.V. Gr./285	sed. surf./rec.	Oslo Fjord	59.1	10.8	49	M
821-13/Q	571-1/JAGO/100	1	Oslo Fjord	59.1	10.8	225	M
821-13 wpr/Q	575-2/GC/99	1	Oslo Fjord	59.1	10.8	173	M
488-12/M	575-2/GC/99	12	Oslo Fjord	59.1	10.8	39	M
488-12/Q	576-1/GC/101	12	Oslo Fjord	59.1	10.8	155	Q
498/M	576-1/GC/101	134	Oslo Fjord	59.1	10.8	31	M
494-12/M	576-1/GC/101	212	Oslo Fjord	59.1	10.8	42	M
494-12/Q	576-1/GC/101	212	Oslo Fjord	59.1	10.8	209	Q

[a]The bdl denotes below detection limit, and wpr denotes whole procedure blank, heterogeneity, and ^{232}Th correction test; all uncertainties are presented at two SEM levels. The $\delta^{234}U_{(0)}$ value represents the originally today measured ($^{234}U/^{238}U$) activity ratio, given in delta notation ($\delta^{234}U(0) = ((^{234}U_{act}/^{238}U_{act}) - 1) \times 1000$). Displayed $\delta^{234}U_{(T)}$ values reflect the age-corrected ($^{234}U/^{238}U$) activity ratios by recalculating the decay of ^{234}U for the time interval T ($\delta^{234}U(T) = \delta^{234}U_{(0)} \times \exp(\lambda^{234} \cdot T)$), determined from $^{230}Th/^{234}U$ age of each individual sample. All errors are deduced on 2σ level.

for U and Th and a $^{230}Th/^{232}Th$ activity ratio of 0.75 ± 0.2, according to *Wedepohl* [1995]. The latter correction appears to be negligible due to sufficiently high $^{230}Th/^{232}Th$ activity ratios and relatively low Th concentrations. Modern scleractinian cold-water corals reveal $\delta^{234}U_{(0)}$ values of 145.5 ± 2.3‰ [*Cheng et al.*, 2000b] and 146.3 ± 3.9‰ [*Liebetrau et al.*, 2010]. We refer to the approach of *Wienberg et al.* [2010, and references therein] to consider samples of a $\delta^{234}U_{(T)}$ value of 146‰ ± 10‰ (modern seawater [*Henderson and Anderson*, 2003]) as reliable, which is apparently only for sample 822-13, not the case ($\delta^{234}U_{(t)} = 246.52 \pm 14.19$) (Table 1).

2.2. Elemental Ratios (Ba/Ca, U/Ca, Li/Ca, and Mg/Ca)

Elemental ratios were measured on a quadrupole ICP-MS Agilent Series 7200cs (GEOMAR) and Thermo X-series II quadrupole ICP-MS at University of Western Australia (UWA). Fossil samples were analyzed at GEOMAR, and the living modern samples were analyzed at UWA. Solutions were analyzed for elemental ratios according to the method of *Rosenthal et al.* [1999]. In particular, elemental ratios were calibrated against multielement standards made from single-element solutions. For comparison, the *Porites* coral powder reference material JCp-1 was analyzed at both labs and yielded the expected absolute ratios and uncertainties presented by *Hathorne et al.* [2013], reflecting both interlaboratory consistency and the robustness of this coral standard. Typical reproducibility (2 standard deviations) is 1.2% for Mg/Ca, 5% Li/Ca, 10% Ba/Ca, and 1.2% U/Ca.

2.2.1. Ba/Ca Ratios

Open ocean dissolved barium has a similar distribution as nutrient and silicate concentrations [*Chan et al.*, 1977] and short residence time of 9 ka [*Broecker and Peng*, 1982]. The use of Ba as a paleo-proxy has been discussed controversial [*McManus et al.*, 1998]. However, in marginal seas and close to rivers, Ba/Ca has been

Table 1. (continued)

^{238}U Concentration (μg/g)			^{232}Th Concentration (ng/g)			(^{230}Th/^{232}Th)			(^{230}Th/^{234}U)			∂^{234}U (0)			∂^{234}U (*t*)			Age (ka)		
2.43	±	0.01	b. d. l.	±	-	b. d. l.	±	-	0.00015	±	0.00004	143	±	4	143	±	4	0.02	±	0.01
4.39	±	0.03	2.99	±	0.24	344.4	±	28.5	344.4	±	28.5	144	±	10	147	±	10	7.5	±	0.2
2.89	±	0.01	0.55	±	0.02	1626.5	±	0.001	0.0883	±	0.0010	142	±	4	146	±	4	10.1	±	0.1
3.10	±	0.02	1.38	±	0.19	712.9	±	101.1	0.0895	±	0.0014	151	±	7	155	±	7	10.2	±	0.2
3.10	±	0.03	1.34	±	0.08	709.8	±	45.4	0.0877	±	0.0021	142	±	13	146	±	14	10.0	±	0.3
6.09	±	0.03	47.41	±	0.28	25.4	±	0.2	0.0570	±	0.0007	137	±	5	139	±	5	6.4	±	0.1
6.06	±	0.14	44.81	±	0.93	27.6	±	3.2	0.0571	±	0.0025	127	±	33	129	±	33	6.4	±	0.3
4.84	±	0.03	1.94	±	0.25	582.9	±	77.3	0.0662	±	0.0021	147	±	9	150	±	9	7.5	±	0.2
5.40	±	0.06	12.41	±	0.81	96.9	±	7.0	0.0630	±	0.0023	141	±	17	144	±	17	7.1	±	0.3
4.52	±	0.06	3.92	±	0.31	277.4	±	23.1	0.0682	±	0.0022	146	±	18	150	±	18	7.7	±	0.3
4.11	±	0.03	1.85	±	0.10	545.1	±	29.0	0.0699	±	0.0010	140	±	11	143	±	11	7.9	±	0.1
3.96	±	0.03	4.28	±	0.50	244.1	±	28.9	0.0751	±	0.0020	141	±	10	144	±	10	8.5	±	0.2
4.33	±	0.02	4.67	±	0.10	260.7	±	8.6	0.0796	±	0.0020	148	±	4	152	±	5	9.0	±	0.2
4.70	±	0.03	5.86	±	0.13	217.8	±	5.3	0.0777	±	0.0010	135	±	8	139	±	8	8.8	±	0.1
3.33	±	0.02	10.48	±	0.34	85.1	±	3.5	0.0764	±	0.0022	133	±	11	136	±	11	8.7	±	0.3
3.50	±	0.02	2.16	±	0.12	515.2	±	29.7	0.0903	±	0.0011	147	±	10	152	±	10	10.3	±	0.1
8.28	±	0.04	5.39	±	0.19	235.2	±	8.8	0.0433	±	0.0005	148	±	4	150	±	4	4.8	±	0.1
4.56	±	0.03	1.66	±	0.02	625.8	±	7.9	0.0656	±	0.0008	131	±	8	134	±	8	7.4	±	0.1
2.83	±	0.01	b. d. l.	±	-	b. d. l.	±	-	0.0001	±	0.0001	146	±	5	146	±	5	0.02	±	0.01
3.29	±	0.01	b. d. l.	±	-	b. d. l.	±	-	0.0002	±	0.0001	145	±	4	145	±	4	0.02	±	0.01
3.52	±	0.02	1.27	±	0.05	402.2	±	15.9	0.0416	±	0.0005	139	±	5	140	±	5	4.6	±	0.1
3.54	±	0.02	10.54	±	0.19	50.0	±	2.0	0.0418	±	0.0015	141	±	7	143	±	7	4.7	±	0.2
4.35	±	0.03	2.16	±	0.01	101.0	±	1.4	0.0143	±	0.0002	142	±	7	143	±	7	1.58	±	0.02
4.24	±	0.04	2.30	±	0.04	98.6	±	2.5	0.0148	±	0.0004	168	±	13	168	±	13	1.63	±	0.04
4.26	±	0.02	44.76	±	0.31	9.1	±	0.1	0.0252	±	0.0007	140	±	3	141	±	3	2.78	±	0.08
4.33	±	0.03	7.27	±	0.05	64.7	±	0.8	0.0309	±	0.0004	145	±	6	146	±	6	3.4	±	0.1
4.22	±	0.05	7.49	±	0.24	65.0	±	5.8	0.0317	±	0.0017	170	±	18	172	±	18	3.51	±	0.2

successfully used as a tracer for fluctuating terrigenous input [e.g., *Bahr et al*., 2013; *Hoffmann et al*., 2014; *Weldeab et al*., 2007] and for tracing meltwater fluxes [*Hall and Chan*, 2004]. Ba/Ca can also be applied to scleractinian warm-water corals [e.g., *Lavigne et al*., 2016; *Sinclair and Mcculloch*, 2004] and cold-water corals [*Anagnostou et al*., 2011; *Montagna et al*., 2005; *Raddatz et al*., 2014a]. The study by *Anagnostou et al*. [2011] is to our knowledge the only existing CWC (scleractinian) calibration for estimating Ba/Ca partition coefficients between seawater and coral aragonite, but was measured in the solitary slow growing *Desmophyllum dianthus*, hence may not be directly applicable to the fast-growing reef-forming CWC, *L. pertusa*. Here we use the Ba/Ca record to infer relative trends of terrigenous input into the coral reef accompanied by meltwater fluxes at sea surface.

2.2.2. Li/Mg Ratios

The Li/Mg ratios were calculated from the Mg/Ca and Li/Ca ratios. The Li/Mg ratio has previously been shown to serve as a robust temperature proxy in scleractinian cold-water corals [*Case et al*., 2010; *Raddatz et al*., 2013; *Montagna et al*., 2014]. Here we use the multispecies calibration of *Montagna et al*. [2014] to calculate bottom water temperatures (BWTs) with the following equation: $Li/Mg_{coral} = 5.41 \exp(-0.049 \times BWT)$, with a resulting uncertainty of ±0.8°C.

Lithium and magnesium are conservative in the ocean and have a residence time of about 1 and 10 Myr, respectively [*HuH et al*., 1998; *Berner and Berner*, 1996]. It has been shown that Li/Ca and Mg/Ca twofold increase over the last 2–3 Myr [*Hathorne and James*, 2006; *Fantle and DePaolo*, 2006], largely reflecting the shorter residence time of Ca compared to Mg (and Li). However, considering the relatively long residence time of Mg and hence Li in the oceans, changes in the Li/Mg ratio of seawater are likely to be minimal even on the time scale of 10^7 years. Accordingly, given that we have reconstructed environmental changes only over the last 11 kyr, we consider seawater changes in Li/Mg as not being relevant.

2.2.3. U/Ca Ratios

Recent studies have shown that U/Ca ratios in scleractinian corals can be used to reconstruct changes in the carbonate system of the ocean [*Anagnostou et al*., 2011; *Inoue et al*., 2011; *Raddatz et al*., 2014b]. There is an

ongoing discussion whether U/Ca ratios of aragonite precipitates reflect seawater pH and/or the carbonate ion concentration (CO_3^{2-}) [*DeCarlo et al.*, 2015]. In the seawater carbonate system, carbonate ion concentration generally decreases with decreasing seawater pH. As all prior U/Ca studies reveal that U/Ca ratios increase with either decreasing seawater pH or carbonate ion concentration, this parameter appears to be largely controlled by seawater carbonate chemistry.

Here we use the U/Ca-seawater pH relationship of *Raddatz et al.* [2014b] with the following equation: $pH_{seawater} = (U/Ca_{Lophelia} - 16.18)/-1.82$, with a relatively large uncertainty of ±0.15 for the reconstructed seawater pH. However, we caution that U/Ca-based seawater pH reconstructions might be biased by potentially large differences in growth or precipitation rates [*Raddatz et al.*, 2014b]. Given these uncertainties, we followed a conservative and more robust approach by mainly focusing on trends rather than absolute seawater pH values.

The residence time of U is calculated to be 200–400 kyr and is therefore considered to be of minor importance controlling U/Ca variations in our record [e.g., *Ku et al.*, 1977; *Henderson*, 2002; *Chabaux et al.*, 2003; *Dunk et al.*, 2002].

For comparison, modern in situ seawater pH and BWT values of the Oslo fjord and Sula reef were taken from *Flögel et al.* [2014]. For the Lopphavet CWC reef BWT were taken from *Raddatz et al.* [2013], but measured seawater pH values are unavailable and were calculated from the CARINA data set by using CO2SYS [*Lewis and Wallace*, 1998] and are therefore probably not as accurate as the in situ measured values (Table 3).

2.2.4. Boron Isotope Measurements

Samples were processed for boron isotope analysis and measured on an NU Plasma II MC-ICP-MS at the University of Western Australia following the protocols of *McCulloch et al.* [2014]. Briefly, for this study, about 5 mg of sample material was used for each determination. All samples were measured in duplicate, except for sample 809-13. Generally, ^{11}B was measured with a signal intensity of approximately 1.5 V.

The boron method is based on a gravimetrically prepared laboratory standard, UWA24.7, calibrated against the international reference standard NIST-SRM 951 ($\delta^{11}B = 0‰$). UWA24.7 standard solutions between 50 to 500 ppb, equivalent to coral sites samples between 2 and 10 mg, exhibit consistent results for $\delta^{11}B$ (24.7 ± 0.3‰ 2σ). The reproducibility of this method ranges from ±0.44 to 0.08‰, for solutions between 50 to 300 ppb, respectively, equivalent to 2–10 mg size coral samples. The external reproducibility of this method is demonstrated by the repeated measurements of the international carbonate standard JCp-1 $\delta^{11}B = 24.3 \pm 0.34‰$ (2 standard deviations), which is consistent with the reported value of 24.2 ± 0.35‰ by the boron isotope interlaboratory comparison project [*Gutjahr et al.*, 2014].

Boron isotopes are most commonly used for reconstructing ambient seawater pH from foraminifera [e.g., *Hönisch et al.*, 2009; *Rae et al.*, 2011; *Foster et al.*, 2012]. Boron isotope compositions of scleractinian cold-water corals, however, appear to record the internal pH of the calcifying fluid of the coral (pH_{cf}), which is up-regulated by physiological processes and strongly correlated to changes in ambient seawater saturation [*McCulloch et al.*, 2012]. In particular, pH up-regulation is enhanced with decreasing seawater saturation state/seawater pH. Here we exploit this to calculate the internal pH_{cf} of the coral by using the equation of *Zeebe and Wolf-Gladow* [2001] based on the measured $\delta^{11}B_{carb}$ in the coral:

$$pH_{cf} = pK_B - \log\left\{\left[\delta^{11}B_{sw} - \delta^{11}B_{carb}\right]/\left[\alpha_{(B3\text{-}B4)}\delta^{11}B_{carb} - \delta^{11}B_{sw} + 1000\left(\alpha_{(B3\text{-}B4)} - 1\right)\right]\right\},$$

where $\delta^{11}B_{carb}$ represents the measured $\delta^{11}B$ value, α is the isotopic fractionation factor between the boric and borate species, and $\delta^{11}B_{sw}$ is the boron isotopic composition of seawater (=39.61 [*Foster et al.*, 2010]). In seawater, boron exists as (1) the tetrahedrally coordinated borate [$B(OH)_4^-$] ion and (2) as the trigonal boric acid [$B(OH)_3$] with a fractionation factor of 27.2‰ ($=\alpha_{(B3\text{-}B4)} = 1.0272$ [*Klochko et al.*, 2006]). Marine calcifiers appear to exclusively incorporate the borate ion into their aragonite skeleton during calcification. A pK_B value of 8.597 is the stoichiometric dissociation constant for boric acid at 25°C and salinity of 35. In principle, pK_B is temperature, salinity, and pressure dependent, but the effect of these parameters is considerably small [*Foster et al.*, 2012].

Furthermore, we calculate the difference between the $\delta^{11}B$-derived pH_{cf} values and the reconstructed seawater pH, where $\Delta pH = pH_{cf} - pH_{sw}$, to quantify coral pH up-regulation as well as the physiological stress

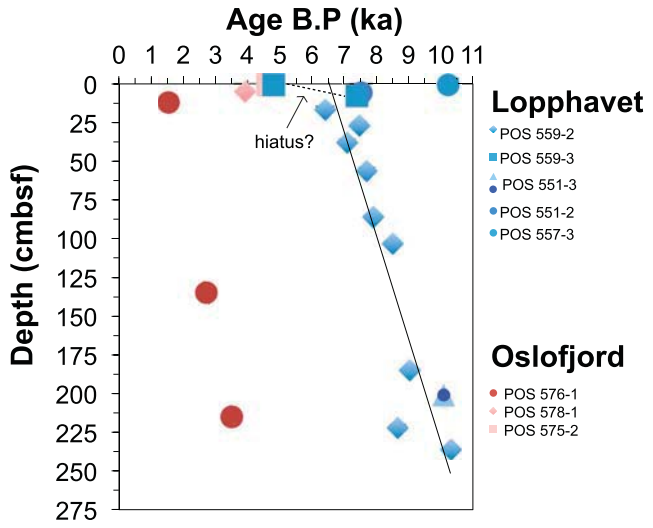

Figure 2. U/Th ages determined in *L. pertusa* samples from various sediment cores from Lopphavet and Oslofjord reef. Note that sediment cores 559-2 and 559-3 are neighboring cores, but only core 559-3 reveals a possible hiatus between 1 and 8 cm. Considering all investigated samples no coral ages were found between 6.4 and 4.8 ka.

on the coral/reef. The ΔpH was determined using a combination of U/Ca (=seawater pH) and $\delta^{11}B$ (=calcifying fluid pH) analyses.

3. Results

3.1. Stratigraphic Constraints

The U/Th age determinations reveal that our coral samples are Holocene in age, ranging from 10.3 ka to 4.6 ka for the Lopphavet cores and ~4.6–1.6 ka for the Oslo fjord (Figure 2 and Table 1). The Lopphavet reef core 559-2 shows an almost continuous record from 10.3 ka to 6.4 ka and hence a sedimentation rate of 55 cm/kyr, apparently slower than >100 cm/kyr reported for other CWC reefs on the Norwegian shelf [*López Correa et al.*, 2012; *Titschack et al.*, 2015]. Furthermore, the nearby core 559-3 (a few hundred meters away) indicates a gap of ~2.6 kyr, from 7.4 to 4.8 ka between 1 and 8 cm core depth. Combining the results of core 559-2 and 559-3, the gap can be reduced to ~1.6 kyr, from 6.4 to 4.8 ka, for this site (Figure 2).

The Oslofjord core 576-1 also shows a relatively continuous record from 3.5 ka to 1.6 ka, and an accumulation rate of 95 cm/kyr, significantly faster than at Lopphavet but similar to the reefs cited above (Figure 2). Core top (1 cm and 5 cm) dating of cores 578-1 and 575-2 reveals ages of 3.53 ka ± 0.02 and 4.64 ka ±0.03, respectively (Figure 2 and Table 1). At 4.74 ka, growth at Oslofjord reef appears to have been reinitiated

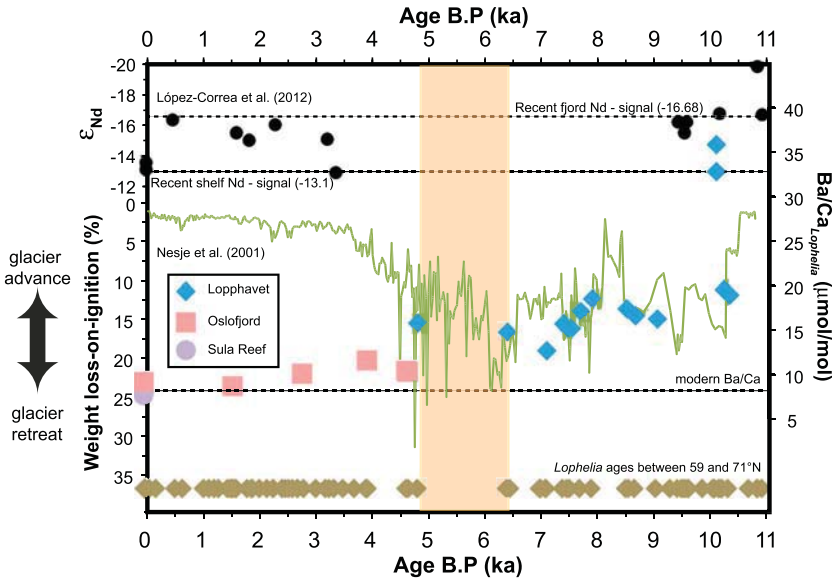

Figure 3. *Lophelia*-Ba/Ca record from Lopphavet and Oslofjord reef covering the last 10.3 kyr. Also plotted are the neodymium isotope record (ε_{Nd}; error bars are smaller than the black dots) of *L. pertusa* from Stjernsund [*López Correa et al.*, 2012] and the weight-loss-on-ignition record from lacustrine sediments (green) [*Nesje et al.*, 2001]. Additionally, a comprehensive plot of published *L. pertusa* ages of the Norwegian margin [*Mikkelsen et al.*, 1982; *López Correa et al.*, 2012; *Lindberg and Mienert*, 2005; *Titschack et al.*, 2015; *Hovland et al.*, 1998; *Hovland and Mortensen*, 1999] is integrated, including North Scottland data [*Douarin et al.*, 2013]. The colored vertical bar marks the interval with no identified coral emplacement so far.

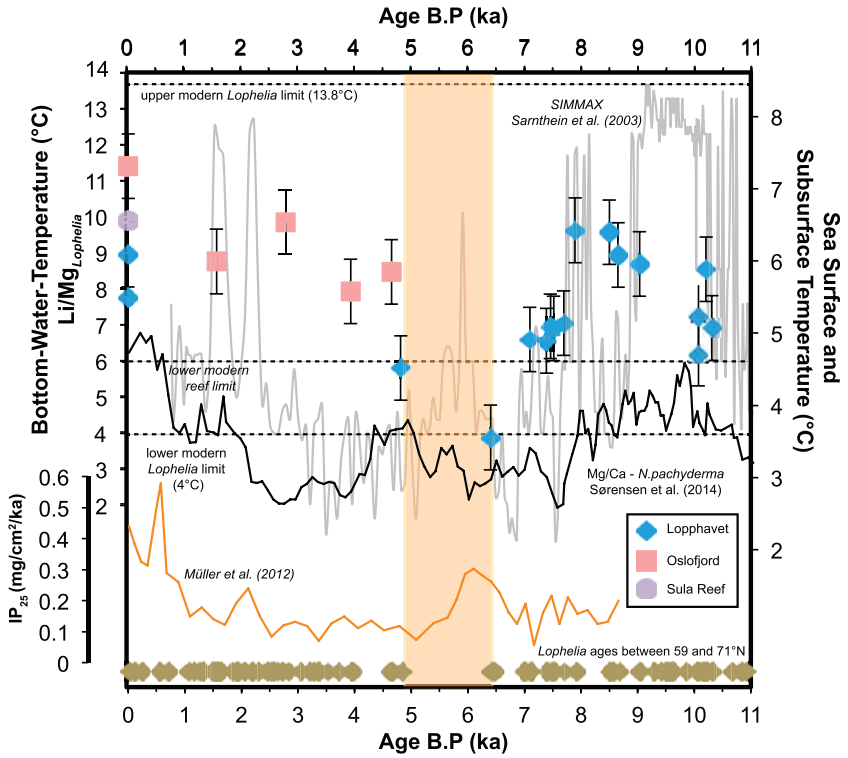

Figure 4. Bottom water temperature (BWT) record based on Mg/Li ratios measured in *L. pertusa* samples. Also plotted are the discussed records of SST (SIMMAX site 23258-2 [*Sarnthein et al.*, 2003]), sub-SST (Mg/Ca *N. pachyderma*, site MSM 5/5 712/2 , *Sørensen et al.* [2014]), and sea ice formation (IP25 [*Müller et al.*, 2012]). *Lophelia* ages and yellow interval are plotted as in Figure 3.

simultaneously with the Lopphavet and Stjernsund reefs [*López Correa et al.*, 2012] in northern Norway. Our new age constraints confirm previous results of earlier studies that showed no CWC growth between 6.4 and 4.8 ka (Figures 2–5) [*Mikkelsen et al.*, 1982; *Hovland et al.*, 1998; *Hovland and Mortensen*, 1999; *Lindberg and Mienert*, 2005; *López Correa et al.*, 2012; *Douarin et al.*, 2013; *Titschack et al.*, 2015].

3.2. Ba/Ca Ratios

The Ba/Ca ratios measured in one modern and one fossil coral reveal only small variations of sample heterogeneity. In particular, the modern sample shows Ba/Ca values for the COC of 7.74 µmol/mol and 8.49 µmol/mol for the theca wall, and the fossil sample shows 35 µmol/mol for the COC and 32 µmol/mol for the theca wall and thus showing only small sample heterogeneity.

The Ba/Ca_{coral} record from Lopphavet reef reaches a maximum of 32 µmol/mol (fibrous aragonite/none COC) at 10.1 ka, which is followed by a decreasing trend toward 6.4 ka (Figure 2). This trend is characterized by short-term variations between 19 and 12 µmol/mol from peak to peak within 2 kyr, which is greater than the determined sample heterogeneity. The overall decreasing trend toward the Holocene is consistent with the Ba/Ca ratios of core 576-1 from the Oslofjord from 12 to 9.2 µmol/mol (Figure 3 and Table 2).

3.3. Li/Mg-Derived Bottom Water Temperatures

The Li/Mg ratios of the entire record range between 2.12 and 4.48 mmol/mol. The BWT temperatures calculated from these Li/Mg ratios (Table 2 and Figure 4) range between 4°C and 13°C $_{(Li/Mg)}$ for the whole sample set, which appears to be within the reported tolerance range of single *L. pertusa* specimens [*Freiwald et al.*, 2004]. At Lopphavet, $BWT_{(Li/Mg)}$ range between 4 and 10°C and reveal an increasing trend from 6.9°C at 10.3 ka to 9.6°C around 7.89 ka, which is followed by an abrupt decrease in $BWT_{(Li/Mg)}$ to 4°C at 6.4 ka at the observed sedimentary gap (Figure 4 and Table 2). The live collected *L. pertusa* specimen represents $BWT_{(Li/Mg)}$ around 8.9°C, which is higher then the measured ambient $BWT_{(Li/Mg)}$ of 7.1°C_{sw} at Lopphavet reef. However, assuming the annual variability is 1.5°C and the uncertainty of ±0.8°C for Li/Mg temperatures [*Montagna et al.*, 2014], the values are in close agreement. Similar small temperature offsets were determined

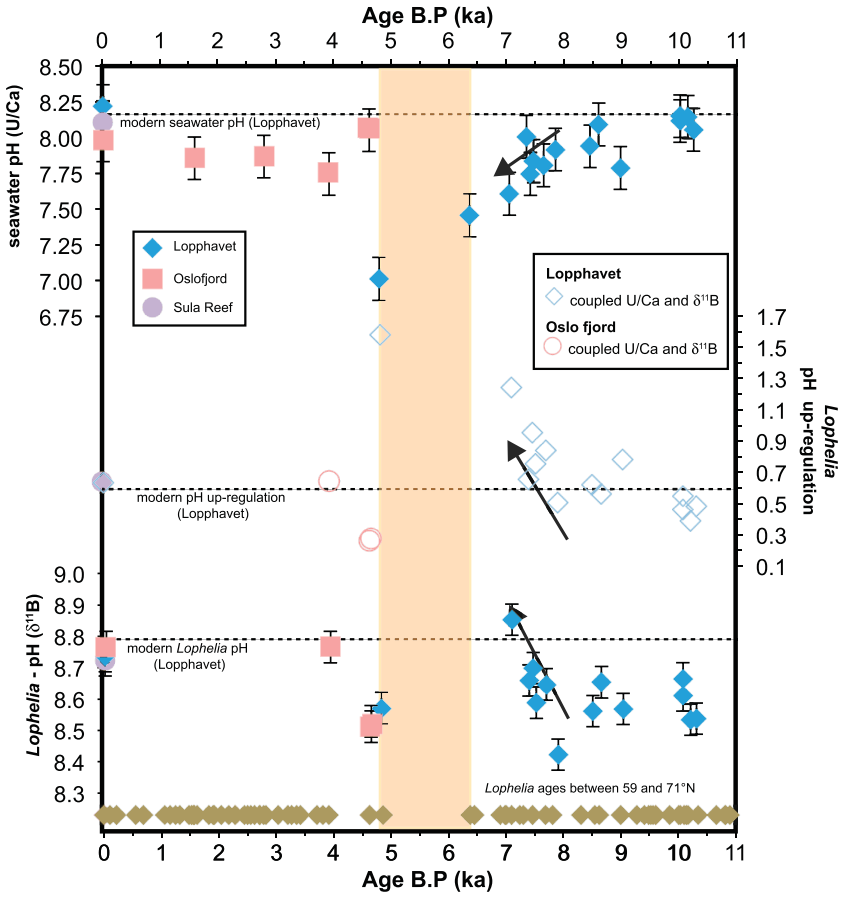

Figure 5. Carbonate system parameter records of seawater pH (based on U/Ca µmol/mol ratios), internal coral pH (based on $\delta^{11}B$), and pH up-regulation (based on coupled $\delta^{11}B$ and U/Ca ratios) covering the last 10.3 kyr. For calculation details see text. *Lophelia* ages and yellow interval are plotted as in Figure 3.

for the live collected *L. pertusa* samples and ambient seawaters of Sula reef (9.9°C $_{(Li/Mg)}$ versus 7.4°C $_{(amb)}$) and Oslofjord (11°C $_{(Li/Mg)}$ and 8.1°C $_{(amb)}$) (Figure 4). Nevertheless, we observe an apparent difference between the Li/Mg ratios of *Lophelia* samples collected from Sula reef and Oslofjord between of our study and previous studies [*Raddatz et al.*, 2013; *Montagna et al.*, 2014] of up to 0.44 mmol/mol for the Oslofjord and 0.1 mmol/mol for the Sula reef. This observation can be explained by a stronger seasonal variation within the Oslofjord compared to the Sula reef. The Oslofjord $BWT_{(Li/Mg)}$ record ranges between 8°C and 13°C, which in terms of variability (i.e., 5°C) is very similar to the Lopphavet $BWT_{(Li/Mg)}$ record (6°C) albeit with significantly higher temperatures. These large-temperature variations and comparatively higher absolute values at 100 m water depth are consistent with observations recorded by the permanent water monitoring station Torbjornskjaer (www.quamontior.no/ytrOslofjord), in which occasional temperature excursions up to 13°C exist.

3.4. Carbonate System and pH Up-regulation

3.4.1. U/Ca Ratios

The U/Ca ratios vary from 1.22 to 3.61 µmol/mol, which is larger than the variability observed within modern and fossil *L. pertusa* samples (COC versus theca, 1.22 versus 1.43 µmol/mol, and 1.42 versus 1.35 µmol/mol; Table 2) and greater than the previously observed U/Ca variability in modern *L. pertusa* samples [*Raddatz et al.*, 2014b; *Sinclair et al.*, 2006]. If taken at face value the U/Ca-based seawater pH reconstruction ($pH_{U/Ca}$) implies large variations of seawater $pH_{U/Ca}$ between 8.25 and 7.0 for the Lopphavet reef and between 8.07 and 7.76 for the Oslofjord. The recent samples from Oslofjord, Sula, and Lopphavet have $pH_{U/Ca}$ values between 8.22 and 7.98, which is similar (within ±0.1) to modern ambient seawater pH (Figure 5 and Table 2). The Oslofjord seawater $pH_{U/Ca}$ record shows similar values within the given uncertainty of 0.15,

Table 2. Elemental Ratios and Boron Isotopes of *Lophelia pertusa* Samples From Research Cruise POS 391 (lab 1 = GEOMAR and lab 2 = UWA)

Lab Code	Lab	Station	Core Depth	Species	Micropart	Location	Age	Error	Li/Mg (mmol/mol)	U/Ca (μmol/mol)	Ba/Ca (μmol/mol)	$\delta^{11}B$ (‰)	Two SEM
429-11	2	550-1 JAGO dive	modern	*L. pertusa* red	Theca	Lopphavet	0.02	0.00	3.49	1.43	8.49	26.62	0.05
430-11	2	550-1 JAGO dive	modern	*L. pertusa* red	COC	Lopphavet	0.02	0.00	3.70	1.22	7.74	22.65	0.06
808-13	1	551-2	6	*L. pertusa*	Theca	Lopphavet	7.51	0.19	3.86	1.92	15.25	25.60	0.07
439-11	2	551-3	200	*L. pertusa*	Theca	Lopphavet	10.07	0.11	3.99	1.41	32.80	26.13	0.05
440-11	2	551-3	200	*L. pertusa*	COC	Lopphavet	10.07	0.11	3.80	1.35	35.82	25.76	0.05
809-13	1	557-3	1	*L. pertusa*	Theca	Lopphavet	10.20	0.17	3.56	1.36	19.58	25.23	0.05
497-12	1	559-2	17	*L. pertusa*	Theca	Lopphavet	6.40	0.29	4.48	2.61	14.80		
810-13	1	559-2	27	*L. pertusa*	Theca	Lopphavet	7.46	0.24	3.85	2.08	15.24	26.36	0.06
811-13	1	559-2	38	*L. pertusa*	Theca	Lopphavet	7.09	0.26	3.92	2.33	12.70	27.41	0.05
812-13	1	559-2	56	*L. pertusa*	Theca	Lopphavet	7.69	0.25	3.83	1.97	17.14	26.00	0.06
813-13	1	559-2	86	*L. pertusa*	Theca	Lopphavet	7.89	0.11	3.38	1.77	18.59	24.47	0.06
814-13	1	559-2	103	*L. pertusa*	Theca	Lopphavet	8.50	0.23	3.38	1.73	17.45	25.41	0.06
816-13	1	559-2	184	*L. pertusa*	Theca	Lopphavet	9.03	0.23	3.54	2.01	16.28	25.47	0.06
817-13	1	559-2	221	*L. pertusa*	Theca	Lopphavet	8.65	0.25	3.49	1.45	16.67	26.05	0.06
818-13	1	559-2	235	*L. pertusa*	Theca	Lopphavet	10.30	0.13	3.86	1.52	19.00	25.25	0.06
819-13	1	559-3	1	*L. pertusa*	Theca	Lopphavet	4.82	0.06	4.07	3.42	15.80	25.48	0.06
820-13	1	559-3	8	*L. pertusa*	Theca	Lopphavet	7.39	0.09	3.93	1.61	15.75	26.09	0.06
433-11	2	563-1	modern	*L. pertusa*	Theca	Sula	0.02	0.01	3.33	1.43	7.72	26.53	0.06
431-11	2	571-1 JAGO dive	modern	*L. pertusa*	Theca	Oslo Fjord	0.02	0.01	3.09	1.66	9.24	26.82	0.05
821-13	1	575-2	1	*L. pertusa*	Theca	Oslo Fjord	4.63	0.06	2.12	1.49	10.47	25.07	0.06
821-13	1	575-2	1	*L. pertusa*	Theca	Oslo Fjord	4.66	0.17	3.57	1.50	10.38	25.13	0.06
822-13	1	578-1	5	*L. pertusa*	Theca	Oslo Fjord	3.94	0.15	3.67	2.07	11.64	26.83	0.06
488-12	1	576-1	12	*L. pertusa*	Theca	Oslo Fjord	1.58	0.02	3.52	1.88	8.77		
498-12	1	576-1	134	*L. pertusa*	Theca	Oslo Fjord	2.71	0.04	3.34	1.84	10.08		
494-12	1	576-1	214	*L. pertusa*	Theca	Oslo Fjord	3.51	0.19	3.71	1.90	12.24		

whereas the Lopphavet record reveals a distinct decrease of about 0.5 $pH_{U/Ca}$ units to an extremely low $pH_{U/Ca}$ value of ~7.5 between 7.7 ka to 6.4 ka (Figure 5 and Table 2). This trend appears to have continued beyond the gap at 4.82 ka to an even lower seawater $pH_{U/Ca}$ of 7.0. This unrealistically low pH is puzzling especially considering that the reconstructed U/Ca-based seawater $pH_{U/Ca}$ reconstruction for the live in situ collected specimens of *L. pertusa* fit within the uncertainty (±0.15) of the ambient seawater (in situ Table 3) values (Lopphavet: $8.1_{(U/Ca)}$ versus $8.15_{(amb)}$, Sula reef: $8.11_{(U/Ca)}$ versus $8.08_{(amb)}$, and Oslofjord: $7.98_{(U/Ca)}$ versus $7.98_{(amb)}$; Figure 5 and Table 2).

3.4.2. Boron Isotopes

Our live collected *L. pertusa* samples from Lopphavet (429-11), Sula reef (433-11), and Oslo-fjord (431-11) show only small variations from 26.5 to 26.8‰, which according to the ambient seawater pH between 7.98 and 8.16 result in ΔpH values between 0.63 and 0.79 (Figure 5 and Table 2), consistent with the findings of previous studies [*Anagnostou et al*., 2012; *Martin et al*., 2016; *McCulloch et al*., 2012; *Wall et al*., 2015]. In accordance to previous findings [*Blamart et al*., 2007; *Wall et al*., 2015] the $\delta^{11}B$ values of the COCs appear to be lower than in the theca wall (429-11/430-11 modern = 26.62‰ versus 22.65‰, 439-11/440-11 fossil = 26.13‰ versus 25.23‰), even though less pronounced in the fossil sample.

However, future studies should focus on determining more species-dependent $\delta^{11}B$-seawater pH calibrations covering a larger range of seawater pH as well as changes in intracoral heterogeneity of boron isotopic compositions through time.

The boron isotope compositions from the downcore records show an overall relatively large variation from 24.47‰ to 27.41‰ (Figure 5). For Lopphavet reef, variations of 3‰ are almost double that of Oslofjord reef

Table 3. Metadata and Oceanographic and Carbonate System Parameters of the Investigated Lopehlia Reefs[a]

Location	Reference	Longitude/ Latitude	Depth (m)	Temperature (°C)	Salinity (g/kg)	DIC (μmol/kg)	pH	TA (μmol/kg)	Ω_{arag}	pCO_2 (μatm)	HCO_3^- (μmol/kg)	CO_3^{2-} (μmol/kg)
Lopphavet	CARINA	19°51.12′E/71°7.8′N	198	6.24	35.018	2146	8.162	2314	1.79	374.5	2004.6	122.8
Sula reef	*Flögel et al.* [2014]	8°11.40′E/64°08.20′N	312	7.43	35.17	2150	8.08	2314	1.74	424	2006	124
Oslo fjord	*Flögel et al.* [2014]	10°48.00′E/59°08.00′N	100	7	35.1	2170	7.98	2287	1.39	556	2046	97

[a]Note that locations do not represent the exact location of sampling; we try to take the closest as possible.

(1.7‰). The corresponding calculated internal $pH_{\delta 11B}$ varies from 8.4_{δ} to 8.9, similar to those determined by *McCulloch et al.* [2012], but with a tendency toward stronger up-regulation between 7.7 ka and 6.4 ka. The internal coral pH values reveal a similar but opposite pattern to the seawater $pH_{(U/Ca)}$ and the $BWT_{(Li/Mg)}$ record.

The calculated ΔpH (U/Ca-δ^{11}B) values are also similar to those determined by *McCulloch et al.* [2012] for *L. pertusa*, with values ranging from 0.1 to 1.6 (Figure 5). It appears that the ΔpH tends to have increased when ambient seawater pH decreased. This observation is generally consistent with previous studies investigating boron isotope systematics in scleractinian cold-water corals in relation to ambient seawater pH [*Anagnostou et al*., 2012; *McCulloch et al*., 2012].

Moreover, similar to the $BWT_{(Li/Mg)}$ and the seawater $pH_{(U/Ca)}$, the δ^{11}B may also reveal a trend of enhanced internal coral pH up-regulation from 7.7 ka to probably 6.4 ka.

4. Discussion

4.1. Meltwater Control on CWC Reef

Even though the Holocene appears to be a rather stable period, an increasing number of studies indicate that local climatic and oceanographic changes were influential [e.g., *Alley et al*., 1997; *Mayewski et al*., 2004; *Wanner et al*., 2011].

The last deglaciation is characterized by major fluxes in meltwater discharge due to the retreat of ice sheets. This had severe impacts on ocean circulation in the North Atlantic [e.g., *Broecker et al*., 1985; *Hall and Chan*, 2004]. Such meltwater events and the associated terrigenous input led to abrupt changes in salinity, which can be traced by Ba/Ca ratios in marine carbonates [*Hall and Chan*, 2004].

Based on our Ba/Ca record, we infer that Norwegian CWC reefs recorded changes in terrigenous input and/or resulting meltwater discharge, which in turn have been recorded in the coral skeletons. The observed elevated Ba/Ca ratios, especially those of the early Holocene at 10.3 ka and 10.1 ka (Figure 3), are indicative of meltwater discharge. Similar observations have been made using a combined approach of U/Th, ^{14}C, and neodymium isotopes measured in *L. pertusa* skeletons [*López Correa et al*., 2012]. They identified a major preboreal meltwater event in the Stjernsund reef (inner sund system) at 10.7 ka. This could suggest that early Holocene meltwater pulses at sea surface in the fjord may have caused elevated Ba concentrations at the seafloor, as *Hall and Chan* [2004] hypothesized that elevated Ba/Ca ratios are primarily of continental origin. However, the lack of 0.4 kyr suggests that these geochemical indicators were unlikely to have originated from the same source. Elevated Ba/Ca ratios may also have been partly caused by increased freshwater transport from the Arctic Ocean into the North Atlantic [*Hall and Chan*, 2004]; however, from this data set it is not possible to fully resolve the specific sources of Ba.

Furthermore, the observed trends in our Ba/Ca records from Lopphavet and Oslofjord may imply a decreasing influence of glacial fluctuations throughout the Holocene (Figure 3). The Holocene glacial activity on the Fennoscandian Shield was not continuous and reveals a rather stepwise pattern, in which three main phases of glacier expansion can be identified (Figure 2) [*Nesje et al*., 2001]. The terminations of those expansions coincide with the recorded Ba/Ca excursions at Lopphavet (Figure 3). The neoglaciation in the Northern Hemisphere at around 5 ka appears to be rather continuous, suggesting that any meltwater events into the fjord system were weak, which might explain the continuous decreasing Ba/Ca ratios. Glacier expansions [e.g., *Nesje et al*., 2001] and decreasing Ba/Ca ratios appear to be contradictory; however, if extended glaciers were stable and did not trigger meltwater events, increased fluxes of Ba into the fjord system would not be expected. This scenario is consistent with determinations by *Hall and Chan* [2004], who related elevated Ba concentration in the Arctic Ocean to periods of ice sheet retreat and the evolution of the Mackenzie River drainage basin.

The major period of glacial fluctuations occurred between 7 and 4 ka, corresponding to the period when there is an apparent absence of CWCs (i.e., between 6.4 ka and 4.8 ka) on the Norwegian margin. These glacial fluctuations might be associated to the Holocene Climatic Optimum and north-south migrations of the Polar Front [*Jansen et al*., 2016]. Furthermore, this coincidence may imply that, during this period, meltwater discharges resulted in a major decline in the calcification of CWC reefs within this region. Enhanced meltwater

discharges from the Fennoscandian Shield may have strongly influenced the North Atlantic Current (NAC), in which the Norwegian CWC reefs thrived.

Interestingly, the third period of glacial expansion is only delayed by a few 100 years with respect to the Oslofjord reef reinitiation at 4.6 ka, thus highlighting a possible link between the Fennoscandian glaciation and CWC reef growth (Figure 3). This is also apparent by comparing reinitiation of growth at other CWC reefs along the Norwegian margin in the late Holocene. We therefore suggest that CWC regrowth occurred once the ice sheet reached a certain level of stability.

4.2. Advances of Arctic Waters

Paleoceanographic reconstructions reveal that the strength of ocean circulation in the Barents Sea and especially the North Atlantic Current (NAC) in the northern North Atlantic has undergone severe changes during the mid-Holocene [e.g., *Sørensen et al*., 2014; *Ebbesen et al*., 2007; *Husum and Hald*, 2012; *Hald et al*., 2007; *Sarnthein et al*., 2003; *Werner et al*., 2013]. Our Li/Mg-derived BWT reconstructions closely follow the pattern of sea surface temperatures (SSTs; SIMMAX based on faunal assemblage transfer function) and sub-SST (100 m water depth) determined from Mg/Ca ratios of the cold-water planktonic foraminifera *Neogloboquadrina pachyderma* from the Barent Sea (23258-2 [*Sarnthein et al*., 2003]) and off Svalbard (MSM 5/5 712/2 [*Sørensen et al*., 2014, Figure 4]). The consistency of these records therefore suggests that surface to subsurface Arctic Ocean temperatures were in-phase. In particular, these studies show that the early Holocene, high-latitude northern North Atlantic, between 80°N and 75°N, was characterized by rather stable conditions. The mid-Holocene was then interrupted by a major decrease in seawater temperature between 9 ka and 8 ka, which was later followed by a major decrease of about 5°C in SST at 75°N [*Sarnthein et al*., 2003] and about 2°C in sub-SST at 79°N [*Sørensen et al*., 2014, Figure 4]. These data agree with other studies of the North Atlantic, in which advection of North Atlantic Current (NAC) weakened poleward due to decreasing Holocene insolation [*Hald et al*., 2007; *Risebrobakken et al*., 2011], which led to strengthening of the East Greenland Current. Between 6.8 and 5.0 ka, weakening of the NAC is also accompanied by sea ice production, as inferred from the sea ice algal proxy IP_{25} off East Greenland (Figure 4) [*Müller et al*., 2012] and off Svalbard [*Forwick and Vorren*, 2009].

Modern CWC reefs off Norway are generally thriving in waters of the NAC, thus highlighting the importance of the NAC for CWC reef growth [*Dullo et al*., 2008], and reflecting the vulnerability of CWCs to major changes in hydrographic conditions. We therefore hypothesize that prevailing cool conditions combined with enhanced sea ice formation, meltwater discharge, and the postglacial Scandinavian uplift that resulted in a drop in sea level by 45 m [*Hald and Vorren*, 1983; *López Correa et al*., 2012; *Møller*, 1989] caused major changes to the oceanographic setting. This in turn led to the southward migration of the Polar Front and Arctic waters, thus hastening the decline of mid-Holocene CWC reefs (Figure 6).

4.3. Physiological Responses of Cold-Water Corals

The Arctic Ocean is generally considered a sink for atmospheric CO_2 [e.g., *Anderson et al*., 2010; *Jutterström and Anderson*, 2010]. In the Arctic Ocean surface waters ($<$200 m), the combination of anthropogenic CO_2 uptake, sea ice melt, river runoff, and cooling have impacted the carbonate chemistry of those waters [*Anderson et al*., 2010]. This effect can also be amplified in subsurface waters due to the remineralization of organic matter, leading to the release of additional CO_2 thereby reducing seawater pH. This process in turn impedes the ability of scleractinian cold-water corals to calcify [*Guinotte et al*., 2006]. Accordingly, our seawater $pH_{(U/Ca)}$ and internal coral $pH_{(\delta 11B)}$ records suggest that the Holocene was characterized by regional ocean acidification events (Figures 4 and 5). In particular, southward advances of surface and subsurface Arctic waters are recorded in the Barent Sea temperature reconstructions [*Sarnthein et al*., 2003; *Sørensen et al*., 2014] and in our $BWT_{(Li/Mg)}$ reconstructions, which are also accompanied by a major decrease in seawater $pH_{(U/Ca)}$ (Figure 5). These events may also have been amplified by significant fluxes in meltwater into the fjord systems. Meltwater fluxes cause a decrease saturation state Ω_{arag} and hence a decrease in seawater pH, especially given that the Fennoscandian Shield has no significant amount of limestone [*Nordgulen and Andresen*, 2008] to buffer the changes in saturation state. However, this effect might be rather small at 200 m water depth.

Furthermore, our approach not only resolves changes in the carbonate system of ambient seawater near the CWC reefs but also has the ability to set improved constraints on the physiological responses due to a

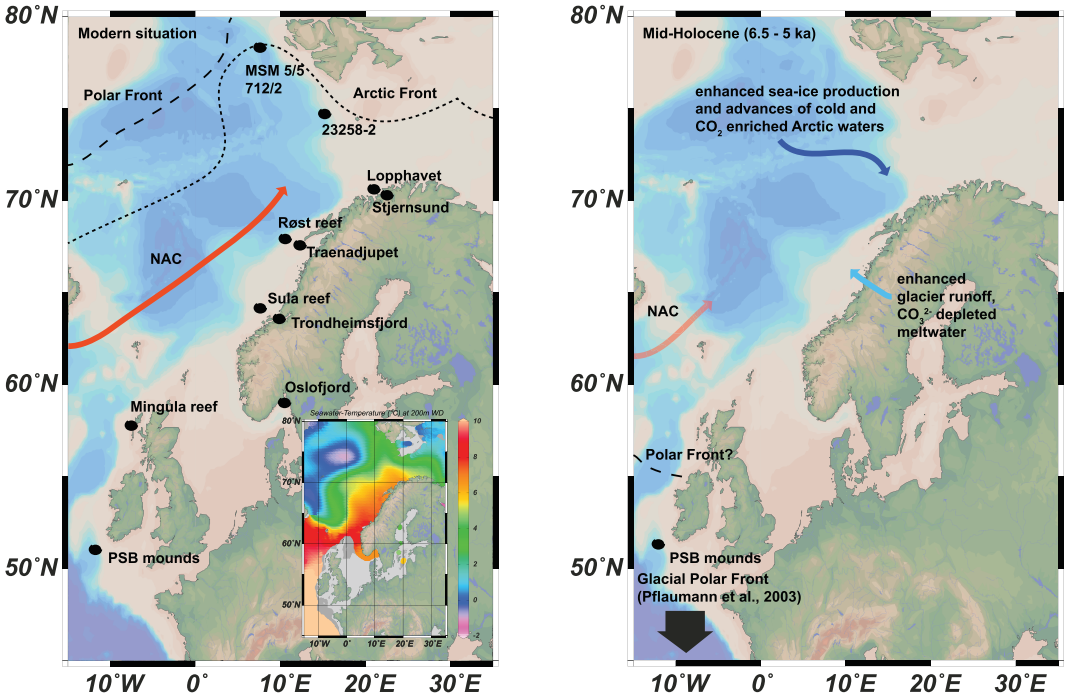

Figure 6. Maps of the northern North Atlantic. (left) The modern situation of flourishing CWC reef on the Norwegian margin. Modern CWC reefs are bathed in the North Atlantic Current (except for the PSB mounds, compare *Dullo et al.* [2008] and *Raddatz et al.* [2014b]) as highlighted in the small map showing the distribution pattern of annual sea surface temperatures based on WOA13 and plotted in ODV [*Schlitzer et al.*, 2014]. Arctic Front and Polar Front boundaries are estimated from REF. Also plotted are locations of the discussed records from sites 23258-2 [*Sarnthein et al.*, 2003] and MSM 5/5 712/2 sub-SST [*Sørensen et al.*, 2014]. (right) Possible scenario for the CWC reef decline between 6.4 ka and 4.8 ka showing enhanced meltwater pulses and the associated weakening of the NAC, the southward migration of the Polar Front, and the resulting advances of cold and pCO_2-rich Arctic waters.

changing saturation state. As recently demonstrated by the application of boron isotopes, scleractinian cold-water corals including *L. pertusa* have the ability to buffer external changes of ambient seawater pH or aragonite saturation, as shown by ΔpH values of 0.7 to 0.9 [*McCulloch et al.*, 2012]. Our coupled δ^{11}B-U/Ca-derived ΔpH reconstructions may show that the reef-forming *L. pertusa* coral responded to changes in ambient seawater by elevating their internal pH, with the additional energy cost likely resulting in the collapse of the reef. In particular, our U/Ca-based seawater pH reconstructions reveal a decrease by up to 0.5 pH units toward the mid-Holocene. According to *McCulloch et al.* [2012], the resultant additional energy cost for *Lophelia* would have been about 50%, which is likely unachievable without additional supply of organic matter. Therefore, we may speculate that these two periods of enhanced pH up-regulation and reef collapse were also characterized by changes in sea surface productivity from which the corals gain their food.

However, the U/Ca-based seawater pH reconstructions might be also biased by other factors such as (1) a changing seawater U/Ca ratio and (2) a growth rate effect on U/Ca ratios.

1. The U/Ca ratio of seawater in oxygenated waters is around 1.305 μmol/mol [*Chen et al.*, 1986] and in scleractinian cold-water corals such *L. pertusa*, typically between 1.0 an 2.0 [e.g., *Raddatz et al.*, 2014; *Sinclair et al.*, 2006], resulting in a distribution coefficient $D = (U/Ca_{sw})/(U/Ca_{Lophelia})$ between 1 and 2. This apparent *D* of greater than 1 reflects the impact of varying seawater U/C_{sw} on coral U/Ca ratios. The input and output factors of U in seawater are not well constrained [e.g., *Henderson*, 2002], but rivers are considered to be the major source and anoxic sediments as the major sink [e.g., *Ku et al.*, 1977; *Henderson*, 2002; *Chabaux et al.*, 2003; *Dunk et al.*, 2002]. Some Norwegian fjords are known for their anoxic conditions in the deeper parts. Accordingly, one may suggest that locally enhanced seawater U concentrations have occurred due to reoxygenation of anoxic U-rich sediments during sea level rise, which finally reached relatively stable conditions at around 6 ka [*Bard et al.*, 1996]. However, Stjernsund never reaches anoxic conditions. Another potential bias for local changes in the U/Ca ratios of seawater could be due to enhanced

terrigenous organic matter fluxes being the carrier phase of authigenic uranium [*Anderson*, 1982; *Zheng et al*., 2002]. Both effects would cause variations of the seawater U/Ca ratio and hence bias seawater pH reconstructions.

2. U/Ca ratios have previously been suggested to be influenced by coral growth rate, where a faster growth rate would result in depleted U/Ca ratios [e.g., *Anagnostou et al*., 2011; *Inoue et al*., 2011; *Sinclair et al*., 2006]. Our ΔpH record would generally be consistent with that proposition given that the coral tends to calcify at a slower rate with increased ΔpH [*McCulloch et al*., 2012]. As an increased pH up-regulation generally results in slower coral growth, we are not able to resolve this question from the present data set.

Nevertheless, consistent with our interpretation, modern oxygenated meltwater incursions into fjord systems have been shown to reduce seawater pH at surface waters to 7.4 [*Pakhomova et al*., 2014], and oceanographic observations by lander system (MoLab) in the Stjernsund CWC reef show pH values as low as 7.6 (S. Flögel, unpublished data). Therefore, we infer from our ΔpH records that there might have been increased stress on the corals that likely resulted in a decline or collapse of CWC reefs, probably along the entire Norwegian margin between 6.4 and 4.8 ka (Figures 5 and 6).

Finally, our results imply that CWCs may be even more susceptible to environmental changes than previously thought; thus, present-day climate change with enhanced CO_2 uptake in the Arctic Ocean may increasingly jeopardize their long-term viability at high latitudes and hence will change the biogeographic limit.

5. Conclusion

This study is based on live collected *L. pertusa* samples and sediment cores retrieved along the Norwegian margin. These may provide evidence that the mid-Holocene CWC reefs recorded major climatic and oceanographic changes that both enhanced CWC reef growth and hastened their regional decline.

1. The analyzed *Lophelia* samples reveal U/Th ages between 10.3 and 6.4 ka for the Lopphavet reef and between 4.6 and 1.5 ka for the Oslofjord reef; yet both reef systems are currently living. Consistent with previous findings, our ages indicate a gap in CWC growth between 6.4 and 4.8 ka, at least for the Lopphavet reef.
2. Ba/Ca ratios analyses of *L. pertusa* from Lopphavet and Oslofjord exhibit similar patterns to Norwegian glacier fluctuations, indicating the influence of meltwater and related Holocene glacier fluctuations on CWC growth.
3. Bottom water temperature reconstruction based on Li/Mg ratios reflects a similar pattern as high-latitude SST and sub-SST records derived from foraminifer Mg/Ca ratios and faunal assemblages, thus implying a strong influence of Arctic waters and a weakening of the NAC, which appear to be amplified by meltwater pulses from the Fennoscandian Shield.
4. Seawater pH reconstructions in CWC reefs appear to show realistic results and therefore confirm the utility of U/Ca as a seawater pH proxy. Large excursions of 0.5 in seawater pH did occur but can be (at least partly) explained by hydrographic changes.
5. We show that coupled U/Ca and $\delta^{11}B$ analyses may be used to constrain physiological controls and in particular, identify periods of enhanced stress on CWCs. We show periods of elevated internal coral pH values together with greater pH up-regulation (ΔpH) in CWC reef-building corals, which probably led to the mid-Holocene collapse of CWC reef between 6.5 and 4.8 ka on the Norwegian margin.

Future studies should aim to clarify whether the mid-Holocene CWC reef decline is an artifact due to the lack of sediment cores or if similar patterns of environmental changes especially to carbonate system parameters are recorded in other CWC reefs.

Acknowledgments

This study is based on material retrieved during research expedition with RV *Poseidon* (POS 391) realized by the DFG project RI 598/4-1. This work benefited from the constructive and valuable comments of one anonymous reviewer and Evan Edinger. We thank the captain, crew, chief scientist Armin Form, and the scientific party of POS 391. J.R. acknowledges funding from DFG project ISOLDE DU 45/1 and 45/3 and ECHO RA 2516-1. S.F. is supported by the German Science Foundation (SFB 754 subproject A7) and the Helmholtz Alliance ROBEX (Robotic Exploration of Extreme Environments). This work would not have been possible without the support of Ana Kolevica. Jan Fietzke is especially acknowledged for providing the Axiom MC-ICP-MS facility on high performance level. The authors further thank Mark Schmidt and Jutta Heinze for their help with the XRD analyses. M.M. and J.T. are supported by the Australian Research Council fellowship FL120100049 and acknowledge support from research project DP0986505. Supporting data can be found as three tables in the paper.

References

Addamo, A. M., A. Vertino, J. Stolarski, R. García-Jiménez, M. Taviani, and A. Machordom (2016), Merging scleractinian genera: The overwhelming genetic similarity between solitary *Desmophyllum* and colonial *Lophelia*, *BMC Evol. Biol.*, *16*, 1–17, doi:10.1186/s12862-016-0654-8.

Alley, R. B., P. A. Mayewski, T. Sowers, M. Stuiver, K. C. Taylor, and P. U. Clark (1997), Holocene climatic instability: A prominent, widespread event 8200 yr ago, *Geology*, *25*, 483–486, doi:10.1130/0091-7613.

Anagnostou, E., R. M. Sherrell, A. Gagnon, M. LaVigne, M. P. Field, and W. F. McDonough (2011), Seawater nutrient and carbonate ion concentrations recorded as P/Ca, Ba/Ca, and U/Ca in the deep-sea coral *Desmophyllum dianthus*, *Geochim. Cosmochim. Acta*, *75*, 2529–2543, doi:10.1016/j.gca.2011.02.019.

Anagnostou, E., K.-F. Huang, C.-F. You, E. L. Sikes, and R. M. Sherrell (2012), Evaluation of boron isotope ratio as a pH proxy in the deep sea coral *Desmophyllum dianthus*: Evidence of physiological pH adjustment, *Earth Plan. Sci. Lett.*, *349–350*, 251–260, doi:10.1016/j.epsl.2012.07.006.

Anderson, R. F. (1982), Concentrations, vertical flux, and remineralization of particulate uranium in seawater, *Geochim. Cosmochim. Acta*, *46*, 1293–1299, doi:10.1016/0016-7037(82)90013-8.

Anderson, L. G., T. Tanhua, G. Björk, S. Hjalmarsson, E. P. Jones, S. Jutterström, B. Rudels, J. Swift, and I. Wahlstöm (2010), Arctic ocean shelf-basin interaction: An active continental shelf CO_2 pump and its impact on the degree of calcium carbonate solubility, *Deep Sea Res., Part I*, *57*, 869–879, doi:10.1016/j.dsr.2010.03.012.

Bahr, A., J. Schönfeld, J. Hoffmann, S. Voigt, R. Aurahs, M. Kucera, S. Flögel, A. Jentzen, and A. Gerdes (2013), Comparison of Ba/Ca and $\delta^{18}O_{WATER}$ as freshwater proxies: A multi-species core-top study on planktonic foraminifera from the vicinity of the Orinoco River mouth, *Earth Plan. Sci. Let.*, *383*, 45–57, doi:10.1016/j.epsl.2013.09.036.

Bard, E., B. Hamelin, A. Maurice, L. Montaggioni, G. Cabioch, G. Faure, and F. Rougerie (1996), Sea level record from Tahiti corals and the timing of deglacial meltwater discharge, *Nature*, *382*, 241–244, doi:10.1038/382241a0.

Blamart, D., C. Rollion-Bard, A. Meibom, J. P. Cuif, A. Juillet-Leclerc, and Y. Dauphin (2007), Correlation of boron isotopic composition with ultrastructure in the deep- sea coral Lophelia pertusa: Implications for biomineralization and paleo-pH, *Geochem. Geophys. Geosyst.*, *8*, doi:10.1029/2007GC001686.

Broecker, W. S., and T.-H. Peng (1982), *Tracers in the Sea*, Lamont-Doherty Earth Observatory, Palisades, New York.

Broecker, W. S., C. Rooth, and T.-H. Peng (1985), Ventilation of the deep northeastern Atlantic, *J. Geophys. Res.*, *90*, 6940–6944, doi:10.1029/JC090iC04p06940.

Berner, E. K., and R. A. Berner (1996), *Global Environment: Water, Air and Geochemical Cycles*, Prentice Hall, Upper Saddle River, N. J.

Case, D., L. F. Robinson, M. E. Auro, and A. C. Gagnon (2010), Environmental controls on Mg and Li in deep-sea scleractinian coral, *Earth Planet. Sci. Lett.*, *300*(3–4), 215–225, doi:10.1016/j.epsl.2010.09.029.

Chan, L. H., D. Drummond, J. M. Edmond, and B. Grant (1977), On the barium data from the Atlantic GEOSECS expedition, *Deep-Sea Res.*, *24*(7), 613–649, doi:10.1016/0146-6291(77)90505-7.

Chabaux, F., J. Riotte, and O. Dequincey (2003), U–Th–Ra fractionation during weathering and river transport, Uranium-Series Geochemistry, *Rev. Mineral. Geochem.*, *52*, 533–576, doi:10.2113/0520533.

Chen, J. H., R. L. Edwards, and G. J. Wasserburg (1986), ^{238}U, ^{234}U, and ^{232}Th in seawater, *Earth Planet. Sci. Lett.*, *80*, 241–251, doi:10.1016/0012-821X(86)90108-1.

Cheng, H., J. F. Adkins, R. L. Edwards, and E. A. Boyle (2000a), U–Th dating of deep-sea corals, *Geochim. Cosmochim. Acta*, *64*, 2401–2416, doi:10.1016/S0016-7037(99)00422-6.

Cheng, H., R. L. Edwards, J. Hoff, C. D. Gallup, D. A. Richards, and Y. Asmerom (2000b), The half-lives of uranium-234 and thorium-230, *Chem. Geol.*, *169*, 17–33, doi:10.1016/S0009-2541(99)00157-6.

DeCarlo, T. M., G. A. Gaetani, M. Holcomb, and A. L. Cohen (2015), Experimental determination of factors controlling U/Ca of aragonite precipitated from seawater: Implications for interpreting coral skeleton, *Geochim. Cosmochim. Acta*, *162*, 151–165, doi:10.1016/j.gca.2015.04.016.

Douarin, M., M. Elliot, S. R. Noble, D. Sinclair, L. A. Henry, D. Long, S. G. Moreton, and J. Murray Roberts (2013), Growth of north-east Atlantic cold-water coral reefs and mounds during the Holocene: A high resolution U-series and ^{14}C chronology, *Earth Plan. Sci. Lett.*, *375*, 176–187, doi:10.1016/j.epsl.2013.05.023.

Douville, E., E. Sallé, N. Frank, M. Eisele, E. Pons-Branchu, and S. Ayrault (2010), Rapid and accurate U-Th dating of ancient carbonates using inductively coupled plasma-quadrupole mass spectrometry, *Chem. Geol.*, *272*, 1–11, doi:10.1016/j.chemgeo.2010.01.007.

Doney, S., V. Fabry, R. Feely, and J. Kleypas (2009), Ocean acidification: The other CO_2 problem, *Annu. Rev. Mar. Sci.*, *1*, 169–192, doi:10.4319/lo.1986.31.5.1122.

Dorschel, B., D. Hebbeln, A. Rüggeberg, W.-C. Dullo, and A. Freiwald (2005), Growth and erosion of a cold-water coral covered carbonate mound in the Northeast Atlantic during Late Pleistocene and Holocene, *Earth Plan. Sci. Lett.*, *233*, 33–44, doi:10.1016/j.epsl.2005.01.035.

Dullo, W. C., S. Flögel, and A. Rüggeberg (2008), Cold-water coral growth in relation to the hydrography of the Celtic and Nordic European continental margin, *Mar. Ecol. Prog. Ser.*, *371*, 165–176, doi:10.3354/meps07623.

Dunk, R. M., R. A. Mills, and W. J. Jenkins (2002), A re-evaluation of the Oceanic Uranium Budget for the Holocene, *Chem. Geol.*, *190*, 45–67, doi:10.1016/S0009-2541(02)00110-9.

Ebbesen, H., M. Hald, and T. H. Eplet (2007), Late glacial and early Holocene climatic oscillations on the western Svalbard margin, European Arctic, *Quat. Sci. Rev.*, *26*, 1999–2011, doi:10.1016/j.quascirev.2006.07.020.

Eisele, M., D. Hebbeln, and C. Wienberg (2008), Growth history of a cold-water coral covered carbonate mound—Galway Mound, Porcupine Seabight, NE-Atlantic, *Mar. Geol.*, *253*, 160–169, doi:10.1016/j.margeo.2010.12.007.

Eisele, M., N. Frank, C. Wienberg, D. Hebbeln, M. López Correa, E. Douville, and A. Freiwald (2011), Productivity controlled cold-water coral growth periods during the last glacial off Mauritania, *Mar. Geol.*, *280*, 143–149, doi:10.1016/j.margeo.2010.12.007.

Fantle, M. S., and D. J. DePaolo (2006), Sr isotopes and pore fluid chemistry in carbonate sediment of the Ontong Java Plateau: Calcite recrystallization rates and evidence for a rapid rise in seawater Mg over the last 10 million years, *Geochim. Cosmochim. Acta*, *70*, 3883–3904, doi:10.1016/j.gca.2006.06.009.

Flögel, S., W.-C. Dullo, O. Pfannkuche, K. Kiriakoulakis, and A. Rüggeberg (2014), Geochemical and physical constraints for the occurrence of living cold-water corals, *Deep Sea Res., Part II*, *99*, 19–26, doi:10.1016/j.dsr2.2013.06.006.

Form, A., and U. Riebesell (2012), Acclimation to ocean acidification during long-term CO_2 exposure in the cold-water coral *Lophelia pertusa*, *Global Change Biol.*, *18*, 843–853, doi:10.1111/j.1365-2486.2011.02583.x.

Frank, N., E. Ricard, A. Lutringer-paquet, C. van der Land, C. Colin, D. Blamart, A. Foubert, D. V. Rooij, and J. P. Henriet (2009), The Holocene occurrence of cold water corals in the NE Atlantic: Implications for coral carbonate mound evolution, *Mar. Geol.*, *266*, 129–142, doi:10.1016/j.margeo.2009.08.007.

Frank, N., et al. (2011), Northeastern Atlantic cold-water coral reefs and climate, *Geology*, *39*(8), 743–746, doi:10.1130/G31825.

Frank, N., M. Paterne, L. Ayliffe, T. van Weering, J. P. Henriet, and D. Blamart (2004), Eastern North Atlantic deep-sea corals: Tracing upper intermediate water $\Delta^{14}C$ during the Holocene, *Earth Planet. Sci. Lett.*, *219*, 297–309, doi:10.1016/S0012-821X(03)00721-0.

Fietzke, J., V. Liebetrau, A. Eisenhauer, and W.-C. Dullo (2005), Determination of uranium isotope ratios by multi-static MIC-ICP-MS: Method and implementation for precise U- and Th-series isotope measurements, *J. Anal. At. Spectrom.*, *20*, 395–401, doi:10.1039/B415958F.

Foubert, A., T. Beck, A. J. Wheeler, J. Opderbecke, A. Grehan, M. Klages, J. Thiede, J.-P. Henriet, and Polarstern ARK-XIX/3a Shipboard Party (2005), New view of the Belgica Mounds, Porcupine, NE Atlantic: Preliminary results from the Polarstern ARK-XIX/3a ROV cruise, in *Cold-Water Corals and Ecosystems*, edited by A. Freiwald and J. M. Roberts, pp. 403–415, Springer, Berlin.

Forwick, M., and T. O. Vorren (2009), Late Weichselian and Holocene sedimentary environments and ice rafting in Isfjorden, Spitsbergen, *Palaeogeogr. Palaeoclim. Palaeoecol.*, *280*, 258–274, doi:10.1016/j.palaeo.2009.06.026.

Foster, G. L., P. A. E. Pogge Von Strandmann, and J. W. B. Rae (2010), Boron and magnesium isotopic composition of seawater, *Geochem. Geophys. Geosyst.*, *11*, Q08015, doi:10.1029/2010GC003201.

Foster, G. L., C. H. Lear, and J. W. B. Rae (2012), The evolution of pCO_2, ice volume and climate during the middle Miocene, *Earth Plan. Sci. Lett.*, *341–344*, 243–254, doi:10.1016/j.epsl.2012.06.007.

Freiwald, A., J. H. Fosså, A. Grehan, T. Koslow, and J. M. Roberts (2004), *Cold-Water Coral Reefs*, vol. 22, 84 pp., UNEP-WCMC Biodiv. Ser., Cambridge.

Freiwald, A., L. Beuck, A. Rüggeberg, M. Taviani, and D. Hebbeln (2009), The white coral community in the central Mediterranean Sea revealed by ROV surveys, *Oceanography*, *22*, 58–74, doi:10.5670/oceanog.2009.06.

Guinotte, J. M., J. Orr, S. Cairns, A. Freiwald, L. Morgan, and R. George (2006), Will human induced changes in seawater chemistry alter the distribution of deep-sea scleractinian corals?, *Front. Ecol. Environ.*, *4*, 141–146, doi:10.1890/1540-9295(2006)004[0141:WHCISC]2.0.CO;2.

Gutjahr, M., et al. (2014), Boron Isotope Intercomparison Project (BIIP): Development of a new carbonate standard for stable isotopic analyses, Geophys. Res. Abstr. EGU Gen. Assembly, 16 (EGU2014-5028-1).

Hald, M., and T. O. Vorren (1983), A shoreline displacement curve from the Tromsø District, North Norway, *Nor. Geol. Tidsskr.*, *63*, 103–110.

Hald, M., C. Andersson, and H. Ebbesen (2007), Variations in temperature and extent of Atlantic water in the northern North Atlantic during the Holocene, *Quat. Sci. Rev.*, *26*, 3423–3440, doi:10.1016/j.quascirev.2007.10.005.

Hall, J. M., and L. H. Chan (2004), Ba/Ca in benthic foraminifera: Thermocline and middepth circulation in the North Atlantic during the last glaciation, *Paleoceanography*, *19*, PA4018, doi:10.1029/2004PA001028.

Hathorne, E., and R. H. James (2006), Temporal record of lithium in seawater: A tracer for silicate weathering?, *Earth Plan. Sci. Lett.*, *246*, 393–406, doi:10.1016/j.epsl.2006.04.020.

Hathorne, E. C., et al. (2013), Inter-laboratory study for coral Sr/Ca and other element/Ca ratio measurements, *Geochem. Geophys. Geosyst.*, *14*, 3730–3750, doi:10.1002/ggge.20230.

Hebbeln, D., D. V. Rooij, and C. Wienberg (2016), Good neighbours shaped by vigorous currents: Cold-water coral mounds and contourites in the North Atlantic, *Mar. Geol.*, *378*, 171–185, doi:10.1016/j.margeo.2016.01.014.

Henderson, G. M. (2002), Seawater ($^{234}U/^{238}U$) during the last 800 thousand years, *Earth Plan. Sci. Lett.*, *199*, 97–110, doi:10.1016/S0012-821X(02)00556-3.

Henderson G. M. and R. F. Anderson (2003), The U-series toolbox for paleoceanography, *Rev. Mineral Geochem.*, *52*, 493–531.

Hoffmann, J., A. Bahr, S. Voigt, J. Schönfeld, D. Nürnberg, and J. Rethemeyer (2014), Disentangling abrupt deglacial hydrological changes in northern South America: Insolation versus oceanic forcing, *Geology*, *42*(7), 579–582, doi:10.1130/G35562.1.

Hönisch, B., N. G. Hemming, D. Archer, M. Siddall, and J. F. McManus (2009), Atmospheric carbon dioxide concentration across the mid-Pleistocene transition, *Science*, *324*, 1551–1554, doi:10.1126/science.1171477.

Hönisch, B., K. A. Allen, A. D. Russell, S. M. Eggins, J. Bijma, H. J. Spero, D. W. Lea, and J. Yu (2011), Planktic foraminifers as recorders of seawater Ba/Ca, *Mar. Micropaleontol.*, *79*, 52–57, doi:10.1016/j.marmicro.2011.01.003.

Hovland, M., and P. B. Mortensen (1999), *Norwegian Coral Reefs and Processes in the Seabed*, John Grieg, Bergen, Norway.

Hovland, M., P. B. Mortensen, T. Brattegard, P. Strass, and K. Rokoengen (1998), Ahermatypic coral banks off mid-Norway: Evidence for a link with seepage of light hydrocarbons, *Palaios*, *13*, 189–200, doi:10.1043/0883-1351(1998)013<0189:ACBOME>2.0.CO;2.

Huh, Y., L. H. Chan, L. Zhang, and J. M. Edmond (1998), Lithium and its isotopes in major world rivers: Implications for weathering and the oceanic budget, *Geochim. Cosmochim. Acta*, *62*, 2039–2051, doi:10.1016/S0016-7037(98)00126-4.

Husum, K., and M. Hald (2012), Arctic planktic foraminiferal assemblages: Implications for subsurface temperature reconstructions, *Mar. Micropaleontol.*, *96–97*, 38–47, doi:10.1016/j.marmicro.2012.07.001.

Jansen, H. L., J. R. Simonsen, S. O. Dahl, J. Bakke, and P. R. Nielsen (2016), Holocene glacier and climate fluctuations of the maritime ice cap Høgtuvbreen, northern Norway, *Holocene*, doi:10.1177/0959683615618265.

Jutterström, S., and L. G. Anderson (2010), Uptake of CO_2 by the Arctic Ocean in a changing climate, *Mar. Chem.*, *122*, 96–104, doi:10.1016/j.marchem.2010.07.002.

Inoue, M., R. Suwa, A. Suzuki, K. Sakai, and H. Kawahata (2011), Effects of seawater pH on growth and skeletal U/Ca ratios of *Acropora digitifera* coral polyps, *Geophys. Res. Lett.*, *38*, L12809, doi:10.1029/2011GL047786.

Kano, A., et al. (2007), Age constraints on the origin and growth history of a deep-water coral mound in the northeast Atlantic drilled during Integrated Ocean Drilling Program Expedition 307, *Geology*, *35*, 1051–1054, doi:10.1130/G23917A.1.

Ku, T. L., K. G. Knauss, and G. G. Mathieu (1977), Uranium in open ocean: Concentration and isotopic composition, *Deep Sea Res.*, *24*, 1005–1017, doi:10.1016/0146-6291(77)90571-9.

Klochko, K., A. J. Kaufman, W. Yoa, R. H. Byrne, and J. A. Tossell (2006), Experimental measurement of boron isotope fractionation in seawater, *Earth Planet. Sci. Lett.*, *248*, 261–270, doi:10.1016/j.epsl.2006.05.034.

Lavigne, M., G. Grottoli, J. E. Palardy, and R. M. Sherrell (2016), Multi-colony calibrations of coral Ba/Ca with a contemporaneous in situ seawater barium record, *Geochim. Cosmochim. Acta*, *179*, 203–216, doi:10.1016/j.gca.2015.12.038.

Lewis, E., and D. W. R. Wallace (1998), Program developed for CO_2 system calculations, ORNL/CDIAC-105, Carbon Dioxide Inf. Anal. Cent. Oak Ridge Natl. Lab., U.S. Dep. of Energy, Oak Ridge, Tenn. [Available at http://cdiac.ornl.gov/oceans/co2rprt.html.]

Liebetrau, V., A. Eisenhauer, and P. Linke (2010), Cold seep carbonates and associated cold-water corals at the Hikurangi margin, New Zealand: New insights into fluid pathways, growth structures and geochronology, *Mar. Geol.*, *272*, 307–318, doi:10.1016/j.margeo.2010.01.003.

Linnaeus, C. (1758), Systema Naturae per regna tria naturae, secundum classes, ordines, genera, species, cum chararteribus, differentiis, synonymis, locis, 10th ed., 824 pp., (Holmiae: Laurentii Salvii), Tomus 1: Regnum Animale, Stockholm.

López Correa, M., P. Montagna, N. Joseph, A. Rüggeberg, J. Fietzke, S. Flögel, B. Dorschel, S. L. Goldstein, A. Wheeler, and A. Freiwald (2012), Preboreal onset of cold-water coral growth beyond the Arctic Circle revealed by coupled radiocarbon and U-series dating and neodymium isotopes, *Quat. Sci. Rev.*, *34*, 24–43, doi:10.1016/j.quascirev.2011.12.005.

Lindberg, B., and J. Mienert (2005), Sedimentological and geochemical environment of the Fugløy Reef off northern Norway, in *Cold-Water Corals and Ecosystems*, pp. 633–650, Springer, Berlin.

Linnaeus, C. (1758), Systema Naturae per regna tria naturae, secundum classes, ordines, genera, species, cum chararteribus, differentiis, synonymis, locis, 10th ed., pp. 824, (Holmiae: Laurentii Salvii), Tomus 1: Regnum Animale, Stockholm.

Martin, P., N. F. Goodkin, J. A. Stewart, G. L. Foster, E. L. Sikes, H. K. White, S. Hennige, and J. M. Roberts (2016), Deep-sea coral $\delta^{13}C$: A tool to reconstruct the difference between seawater pH and $\delta^{11}B$-derived calcifying fluid pH, *Geophys. Res. Lett.*, *43*, 299–308, doi:10.1002/2015GL066494.

Mayewski, P. A., et al. (2004), Holocene climate variability, *Quat. Res.*, *62*, 243–255, doi:10.1016/j.yqres.2004.07.001.
Mcculloch, M. T., M. Holcomb, K. Rankenburg, and J. A. Trotter (2014), Rapid, high-precision measurements of boron isotopic compositions in marine carbonates, Rapid Commun. *Mass. Spectrom.*, 2704–2712, doi:10.1002/rcm.7065.
McCulloch, M., et al. (2012), Resilience of cold-water scleractinian corals to ocean accidification: Boron isotopic systematics of pH and saturation state up-regulation, *Geochim. Cosmochim. Acta*, *87*, 21–34, doi:10.1016/j.gca.2012.03.027.
McCulloch, M. T., M. Taviani, P. Montagna, M. Lopez Correa, A. Remia, and G. Mortimer (2010), Proliferation and demise of deep-sea corals in the Mediterranean during the Younger Dryas, *Earth Planet. Sci. Lett.*, *298*(1–2), 143–152, doi:10.1016/j.epsl.2010.07.036.
McManus, J., et al. (1998), Geochemistry of barium in marine sediments: Implications for its use as a paleo proxy, *Geochim. Cosmochim. Acta*, *62*, 3453–3473, doi:10.1016/S0016-7037(98)00248-8.
Mienis, F., G. C. A. Duineveld, A. J. Davies, M. M. S. Lavaleye, S. W. Ross, H. Seim, J. Bane, and H. van Haren (2014), Cold-water coral growth under extreme environmental conditions, the Cape Lookout area, NW Atlantic, *Biogeosciences*, *11*, 2543–2560, doi:10.5194/bg-11-2543-2014.
Mikkelsen, N., H. Erlenkeuser, J. S. Killingley, and W. H. Berger (1982), Norwegian Corals: Radiocarbon and stable isotopes in *Lophelia pertusa*, *Boreas*, *11*, 163–171, doi:10.1111/j.1502-3885.1982.tb00534.x.
Montagna, P., M. McCulloch, M. Taviani, A. Remia, and G. Rouse (2005), High-resolution trace and minor element compositions in deep-water scleractinian corals (*Desmophyllum dianthus*) from the Mediterranean Sea and the Great Australian Bight, in *Cold-Water Corals and Ecosystems*, edited by A. Freiwald and J. M. Roberts, pp. 1109–1126, Springer, Berlin.
Montagna, P., et al. (2014), Li/Mg systematics in scleractinian corals: Calibration of the thermometer, *Geochim. Cosmochim. Acta*, *132*, 288–310, doi:10.1016/j.gca.2014.02.005.
Møller, J. J. (1989), Geometric simulation and mapping of Holocene relative sea-level changes in northern Norway, *J. Coastal Res.*, *5*(3), 403–417.
Müller, J., K. Werner, and R. Stein (2012), Holocene cooling culminates in sea ice oscillations in Fram Strait, *Quat. Sci. Rev.*, *47*, 1–14, doi:10.1016/j.quascirev.2012.04.024.
Nesje, A., J. A. Matthews, O. Dahl, M. S. Berrisford, and C. Andersson (2001), Holocene glacier fluctuations of Flatebreen and winter-precipitation changes in the Jostedalsbreen region, western Norway, based on glaciolacustrine sediment records, *Holocene*, *11*, 267–280, doi:10.1191/095968301669980885.
Nordgulen, Ø., and A. Andresen (2008), The Precambrian, in *The Making of a Land—Geology of Norway*, edited by I. B. Ramberg et al., pp. 62–119, Norsk Geologisk Forening, Trondheim, Norway.
Pakhomova, S., H. F. V. Braaten, E. Yakushev, and J. Skei (2014), Biogeochemical consequences of an oxygenated intrusion into an anoxic fjord, *Geochem. Trans.*, *15*, 5, doi:10.1186/1467-4866-15-5.
Pflaumann, U., et al. (2003), *Glacial North Atlantic: Sea-surface conditions reconstructed by GLAMAP-2000, Paleoceanography, 18/3, 1065*, doi:10.1029/2002/PA000774.
Rae, J. W. B., G. L. Foster, D. N. Schmidt, and T. Elliott (2011), Boron isotopes and B/Ca in benthic foraminifera: Proxies for the deep ocean carbonate system, *Earth Plan. Sci. Lett*, *302*, 403–413, doi:10.1016/j.epsl.2010.12.034.
Raddatz, J., A. Rüggeberg, S. Margreth, W.-C. Dullo, and IODP Expedition 307 Scientific Party (2011), Paleoenvironmental reconstruction of Challenger Mound initiation in the Porcupine Seabight, NE Atlantic, *Mar. Geol.*, *282*, 79–90, doi:10.1016/j.margeo.2010.10.019.
Raddatz, J., et al. (2013), Stable Sr-isotope, Sr/Ca, Mg/Ca, Li/Ca and Mg/Li ratios in the scleractinian cold-water coral *Lophelia pertusa*, *Chem. Geol.*, *352*, 143–152, doi:10.1016/j.chemgeo.2013.06.013.
Raddatz, J., A. Rüggeberg, V. Liebetrau, A. Foubert, E. Hathorne, J. Fietzke, A. Eisenhauer, and W.-C. Dullo (2014a), Environmental boundary conditions of cold-water coral mound growth over the last 3 million years in the Porcupine Seabight, Northeast Atlantic, *Deep Sea Res., Part II*, *99*, 117–236, doi:10.1016/j.dsr2.2013.06.009.
Raddatz, J., A. Rüggeberg, S. Floegel, E. Hathorne, V. Liebetrau, A. Eisenhauer, and W.-C. Dullo (2014b), The influence of seawater pH on U/Ca ratios in the scleractinian cold-water corals *Lophelia pertusa*, *Biogeosciences*, *11*, 1863–1871, doi:10.5194/bg-11-1863-2014.
Risebrobakken, B., T. Dokken, and L. H. Smedsrud (2011), Early Holocene temperature variability in the Nordic Seas: The role of oceanic heat advection versus changes in orbital forcing, *Paleoceanography*, *26*, PA4206, doi:10.1029/2011PA002117.
Roberts J. M., and S. D. Cairns (2014), Cold-water corals in a changing ocean, *Curr. Opin. Environ. Sustain.*, *7*, 118–126, doi:10.1016/j.cosust.2014.01.004.
Roberts, J. M., A. J. Wheeler, and A. Freiwald (2006), Reefs of the deep: The biology and geology of cold-water coral ecosystems, *Science*, *312*, 543–547, doi:10.1126/science.1119861.
Rosenthal, Y., M. P. Field, and R. M. Sherrell (1999), Precise determination of element/calcium ratios in calcareous samples using sector field inductively coupled plasma mass spectrometry, *Anal. Chem.*, *71*(15), 3248–3253, doi:10.1021/ac981410x.
Rüggeberg, A., W.-C. Dullo, B. Dorschel, and D. Hebbeln (2007), Environmental changes and growth history of a cold-water carbonate mound (Propeller Mound, Porcupine Seabight), *Int. J. Earth Sci.*, *96*, 57–72, doi:10.1007/s00531-005-0504-1.
Rüggeberg, A., J. Fietzke, V. Liebetrau, A. Eisenhauer, W.-C. Dullo, and A. Freiwald (2008), Stable strontium isotopes ($\delta^{88/86}$Sr) in cold-water corals—A new proxy for the reconstruction of intermediate ocean water temperatures, *Earth Planet. Sci. Lett.*, *269*(3–4), 569–574, doi:10.1016/j.epsl.2008.03.002.
Rüggeberg, A., S. Flögel, W. Dullo, K. Hissmann, and A. Freiwald (2011), Water mass characteristics and sill dynamics in a subpolar cold-water coral reef setting at Stjernsund, northern Norway, *Mar. Geol.*, *282*, 5–12, doi:10.1016/j.margeo.2010.05.009.
Rüggeberg, A., S. Flögel, W. Dullo, J. Raddatz, and V. Liebetrau (2016), Paleoseawater density reconstruction and its implication for cold-water coral carbonate mounds in the northeast Atlantic through time, *Paleoceanography*, *31*, 1–15, doi:10.1002/2015PA002859.
Sarnthein, M., S. A. van Kreveld, H. Erlenkeuser, P. M. Grootes, M. Kucera, U. Pflaumann, and M. Schulz (2003), Centennial-to-millennial-scale periodicities of Holocene climate and sediment injections off western Barents shelf, 75°N, *Boreas*, *32*(3), 447–461, doi:10.1111/j.1502-3885.2003.tb01227.x.
Schlitzer, R. (2014), Ocean Data View, [Available at http://odv.awi.de.]
Sinclair, D. J., and M. T. Mcculloch (2004), Corals record low mobile barium concentrations in the Burdekin River during the 1974 flood: Evidence for limited Ba supply to rivers?, *Paleogr. Paleoclim. Paleoceol.*, *214*, 155–174, doi:10.1016/j.palaeo.2004.07.028.
Sinclair, D. J., B. Williams, and M. Risk (2006), A biological origin for climate signals in corals—Trace element "vital effects" are ubiquitous in Scleractinian coral skeletons, *Geophys. Res. Lett.*, *33*, L17707, doi:10.1029/2006GL027183.
Sørensen S. A., K. Husum, M. Hald, T. Marchitto and F. Godtliebsen (2014), Sub sea surface temperatures in the Polar North Atlantic during the Holocene: Planktic foraminiferal Mg/Ca temperature reconstructions, *Holocene*, *24*, 93–103, doi:10.1177/0959683613515730.
Stalder, C., S. Spezzaferri, A. Rüggeberg, C. Pirkenseer, and G. Gennari (2014), Late Weichselian deglaciation and early Holocene development of a cold-water coral reef along the Lopphavet shelf (northern Norway) recorded by benthic foraminifera and ostracoda, *Deep Sea Res., Part II*, *99*, 249–269, doi:10.1016/j.dsr2.2013.07.009.

Trotter, J. A., P. Montagna, M. T. McCulloch, S. Silenzi, S. Reynaud, G. Mortimer, S. Martin, C. Ferrier-Page's, J.-P. Gattuso, and R. Rodolfo-Metalpa (2011), Quantifying the pH "vital effect" in the temperate zooxanthellate coral *Cladocora caespitosa*: Validation of the boron seawater pH proxy, *Earth Plan. Sci. Lett.*, *303*, 163–173, doi:10.1016/j.epsl.2011.01.030.

Titschack, J., D. Baum, R. De Pol Holz, C. M. Lopéz, N. Forster, S. Flögel, D. Hebbeln, and A. Freiwald (2015), Aggradation and carbonate accumulation of Holocene Norwegian cold-water coral reefs, *Sedimentology*, *62*, 1873–1898, doi:10.1111/sed.12206.

Wall, M., F. Ragazzola, L. C. Foster, A. Form, and D. N. Schmidt (2015), PH up-regulation as a potential mechanism for the cold-water coral *Lophelia pertusa* to sustain growth in aragonite undersaturated conditions, *Biogeosciences*, *12*, 6757–6781, doi:10.5194/bg-12-6869-2015.

Wanner, H., O. Solomina, M. Grosjean, S. P. Ritz, and M. Jetel (2011), Structure and origin of Holocene cold events, *Quat. Sci. Rev.*, *30*, 3109–3123, doi:10.1016/j.quascirev.2011.07.010.

Wedepohl, K. H. (1995), The composition of the continental crust, *Geochim. Cosmochim. Acta*, *59*(7), 1217–1232, doi:10.1016/0016-7037(95)00038-2.

Werner, K., R. F. Spielhagen, and D. Bauch (2013), Atlantic Water advection versus sea-ice advances in the eastern Fram Strait during the last 9 ka—Multiproxy evidence for a two-phase Holocene, *Paleoceanography*, *28*, 283–295, doi:10.1002/palo.20028.

Weldeab, S., D. W. Lea, R. R. Schneider, and N. Andersen (2007), 155,000 years of west African monsoon and ocean thermal evolution, *Science*, *316*, 1303–1307, doi:10.1126/science.1140461.

Wienberg, C., D. Hebbeln, H. G. Fink, F. Mienis, B. Dorschel, A. Vertino, and M. Lo (2009), Scleractinian cold-water corals in the Gulf of Cadiz—First clues about their spatial and temporal distribution, *Deep Sea Res., Part I*, *56*, 1873–1893, doi:10.1016/j.dsr.2009.05.016.

Wienberg, C., N. Frank, K. N. Mertens, J. B. Stuut, M. Marchant, J. Fietzke, F. Mienis, and D. Hebbeln (2010), Glacial cold-water coral growth in the Gulf of Cádiz: Implications of increased palaeo-productivity, *Earth Plan. Sci. Lett.*, *298*, 405–416, doi:10.1016/j.epsl.2010.08.017.

Zeebe R., and D. A. Wolf-Gladow (2001), CO_2 in Seawater: Equilibrium, kinetics, isotopes, vol. 65, pp. 346, Elsevier Oceanography Series, Elsevier, Amsterdam.

Zheng, Y., R. F. Anderson, A. Van Geen, and M. Q. Fleisher (2002), Preservation of particulate non-lithogenic uranium in marine sediments, *Geochim. Cosmochim. Acta*, *66*, 3085–3092, doi:10.1016/S0016-7037(01)00632-9.